



CMS-SUS-13-004

CERN-PH-EP/2013-037
2015/03/31

Search for supersymmetry using razor variables in events with b-tagged jets in pp collisions at $\sqrt{s} = 8 \text{ TeV}$

The CMS Collaboration^{*}

Abstract

An inclusive search for supersymmetry in events with at least one b-tagged jet is performed using proton-proton collision data collected by the CMS experiment in 2012 at a center-of-mass energy of 8 TeV. The data set size corresponds to an integrated luminosity of 19.3 fb^{-1} . The two-dimensional distribution of the razor variables R^2 and M_R is studied in events with and without leptons. The data are found to be consistent with the expected background, which is modeled with an empirical function. Exclusion limits on supersymmetric particle masses at a 95% confidence level are derived in several simplified supersymmetric scenarios for several choices of the branching fractions. By combining the likelihoods of a search in events without leptons and a search that requires a single lepton (electron or muon), an improved bound on the top-squark mass is obtained. Assuming the lightest supersymmetric particle to be stable, weakly interacting, and to have a mass of 100 GeV, the branching-fraction-dependent (-independent) production of gluinos is excluded for gluino masses up to 1310 (1175) GeV. The corresponding limit for top-squark pair production is 730 (645) GeV.

Published in Physical Review D as doi:10.1103/PhysRevD.91.052018.

1 Introduction

Supersymmetry (SUSY) is a proposed symmetry of nature that introduces a bosonic (fermionic) partner for every standard model (SM) fermion (boson) [1–9]. Supersymmetric extensions of the SM that include a stable new particle at the electroweak scale are well motivated because they may explain the origin of dark matter. The discovery of the Higgs boson [10–12] at the CERN LHC has renewed interest in “natural” SUSY models, which minimize the fine-tuning associated with the observed value of the Higgs boson mass due to its radiative corrections. In the typical spectrum of these models, the lightest neutralino and chargino are the lightest (LSP) and next-to-lightest (NLSP) SUSY particles, respectively [13–18]. Charginos and neutralinos are fermions, corresponding to a quantum mixture of the SUSY partners of the electroweak and Higgs bosons. The bottom and top squarks are the lightest squarks. The gluino is heavier than these particles but potentially accessible at the LHC. Events are thus characterized by an abundance of jets originating from the hadronization of bottom quarks, a feature that we exploit in this study. Previous searches for natural SUSY by the CMS [19–23] and ATLAS Collaborations [24–28] at the LHC have probed gluino masses up to 1300 GeV and top squark masses up to 700 GeV under the assumptions of specific decay modes for the SUSY particles.

We present an inclusive search for gluinos and top squarks in the context of natural SUSY. Natural SUSY spectra include a gluino, the third-generation squarks, a chargino, and a neutralino, representing the minimum particle content needed in SUSY theories to stabilize the Higgs boson mass. Within the context of natural SUSY, several simplified models [29–34] are considered (Section 2), defined by a specific production mechanism of SUSY particle pairs, with at most two decay channels for each production mode.

The search is performed using events with two or more jets, at least one of which is identified as originating from a bottom quark (jet b tagging). The study is based on the data collected by the CMS Collaboration in proton-proton collisions at $\sqrt{s} = 8$ TeV in 2012, corresponding to an integrated luminosity of 19.3 fb^{-1} . We distinguish the signal from the SM background through their different shapes in the razor variables M_R and R^2 [35, 36]. This search extends the results we presented at 7 TeV [37, 38] using the same analysis procedure. The razor variables have also been used by the ATLAS Collaboration to perform a multi-channel search for SUSY at 7 TeV [39].

The razor variables M_R and R^2 are motivated by the generic process of the pair production of two heavy particles (e.g., squarks or gluinos), each decaying to an undetected particle (the stable, weakly interacting LSP $\tilde{\chi}_1^0$) plus visible particles. The LSP is assumed to escape without detection, leading to an imbalance \vec{p}_T^{miss} in the momentum perpendicular to the beam axis. Each event is treated as a dijet-like event and the four-momenta of the two jets are used to compute M_R and M_T^R , defined as

$$M_R \equiv \sqrt{(|\vec{p}_T^{j_1}| + |\vec{p}_T^{j_2}|)^2 - (p_z^{j_1} + p_z^{j_2})^2}, \quad (1)$$

$$M_T^R \equiv \sqrt{\frac{E_T^{\text{miss}}(p_T^{j_1} + p_T^{j_2}) - \vec{p}_T^{\text{miss}} \cdot (\vec{p}_T^{j_1} + \vec{p}_T^{j_2})}{2}}, \quad (2)$$

where \vec{p}_j , $\vec{p}_T^{j_i}$, and $p_z^{j_i}$ are the momentum of the i th jet, its transverse component with respect to the beam axis, and its longitudinal component, respectively, with E_T^{miss} the magnitude of \vec{p}_T^{miss} . While M_T^R quantifies the transverse momentum imbalance, M_R estimates the mass scale of new-physics particle production in the event. The razor dimensionless ratio is defined as

$$R \equiv \frac{M_T^R}{M_R}. \quad (3)$$

In this search, each event is reduced to a two-jet topology by clustering the selected objects (jets and leptons) into two megajets [36–38]. All possible assignments of objects to the megajets are considered, with the requirement that a megajet consist of at least one object. The sum of the four-momenta of the objects assigned to a megajet defines the megajet four-momentum. When more than two objects are reconstructed, more than one megajet assignment is possible. We select the assignment that minimizes the sum of the invariant masses of the two megajets.

The analysis is performed on several exclusive data sets, referred to as razor boxes, differing in the lepton and jet multiplicity. Each box with fewer than two identified leptons (electrons or muons) is analyzed in exclusive b-tagged jet multiplicity bins in order to maximize the sensitivity to both direct and cascade production of third-generation squarks. For a given box and b-tagged jet multiplicity, the shape of the SM background distribution is evaluated in two rectangular regions of the (M_R, R^2) plane (sidebands), selected so that potential bias due to contributions from signal events is negligible. The background shape is then extrapolated to the signal-sensitive region of the (M_R, R^2) plane. The results are interpreted in the context of several SUSY simplified models by performing a hypothesis test. The test compares the background-only and signal-plus-background possibilities through simultaneous examination of the data in the two sidebands and the signal-sensitive region [40]. In addition, we combine the results from the razor boxes with those from our previous search [19] for top-squark production in the single-lepton (electron or muon) channel to obtain an improved bound on top-squark pair production with respect to previous CMS studies. For this combination, only the razor boxes without an identified lepton (hadronic boxes) are used, so that the event samples from the two studies are mutually exclusive.

This paper is organized as follows. Section 2 presents the spectra of the simplified natural SUSY models examined in this analysis. The CMS detector is briefly described in Section 3. The event selection and razor variables are defined in Sections 4 and 5, respectively. The statistical model used to describe the SM backgrounds as well as the comparisons between the predicted and observed event yields in the search regions are shown in Section 6, followed by a summary of the limit-setting procedure in Section 7. The interpretation of the results and a summary are presented in Sections 8 and 9, respectively.

2 Simplified natural SUSY models

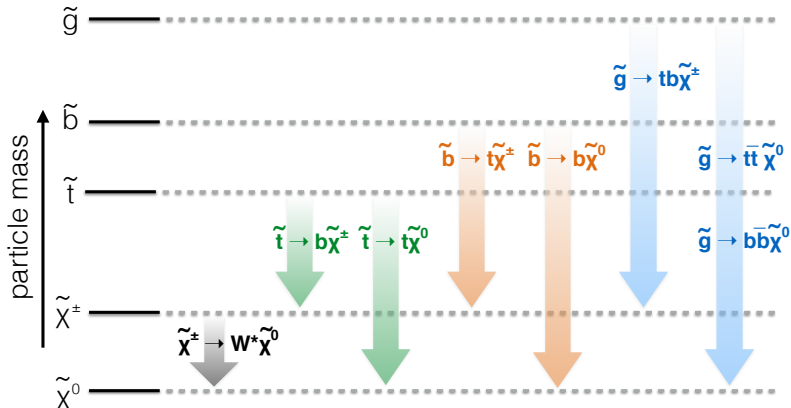


Figure 1: The simplified natural SUSY spectrum considered in this paper, along with the assumed decay modes.

In this paper, natural simplified SUSY scenarios are used to interpret results. The LSP is the lightest neutralino $\tilde{\chi}_1^0$ while the NLSP is the lightest chargino $\tilde{\chi}_1^\pm$. They are both higgsinos and

their mass splitting is taken to be 5 GeV. The NLSP decays to the LSP and a virtual W boson ($\tilde{\chi}_1^\pm \rightarrow W^* \tilde{\chi}_1^0$). The other SUSY particles accessible at the LHC are the gluino and the lightest top and bottom squarks. All other SUSY particles are assumed to be too heavy to participate in the interactions. The SUSY particles and their possible decay modes within this natural SUSY spectrum are summarized in Fig. 1.

In the context of this natural spectrum, five simplified models [29–34] are considered for gluino pair production, based on three-body gluino decays [41]:

- **T1bbbb:** pair-produced gluinos, each decaying with a 100% branching fraction to a bottom quark-antiquark ($b\bar{b}$) pair and the LSP;
- **T1tbbb:** pair-produced gluinos, each decaying with a 50% branching fraction to a $b\bar{b}$ pair and the LSP or to a top quark (antiquark), a bottom antiquark (quark), and the NLSP;
- **T1ttbb:** pair-produced gluinos, decaying with a 100% branching fraction to a top quark (antiquark), a bottom antiquark (quark), and the NLSP;
- **T1tttb:** pair-produced gluinos, each decaying with a 50% branching fraction to a top quark-antiquark ($t\bar{t}$) pair and the LSP or to a top quark (antiquark), a bottom antiquark (quark), and the NLSP;
- **T1tttt:** pair-produced gluinos, each decaying with a 100% branching fraction to a $t\bar{t}$ pair and the LSP.

The corresponding Feynman diagrams are shown in Fig. 2.

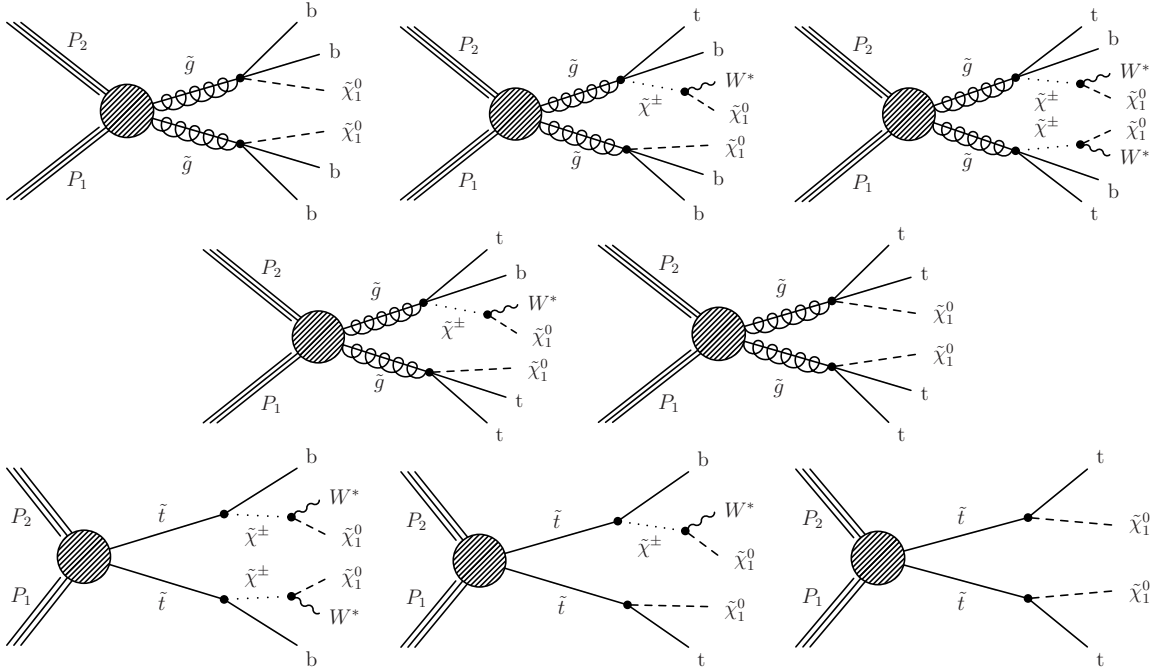


Figure 2: Diagrams displaying the event topologies of gluino (upper 5 diagrams) and top-squark (lower 3 diagrams) pair production considered in this paper.

In addition, the following three simplified models are considered for the production of top-squark pairs:

- **T2bW^{*}:** pair-produced top squarks, each decaying with a 100% branching fraction to a bottom quark and the NLSP;

- **T2tb**: pair-produced top squarks, each decaying with a 50% branching fraction to a top quark and the LSP or to a bottom quark and the NLSP;
- **T2tt**: pair-produced top squarks, each decaying with a 100% branching fraction to a top quark and the LSP.

The corresponding Feynman diagrams are shown in Fig. 2.

Events for the eight simplified models are generated with the MADGRAPH V5 generator [42, 43], in association with up to two partons. The SUSY particle decays are treated with PYTHIA V6.4.26 assuming a constant matrix element (phase space decay). The parton showering is described by PYTHIA and matched to the matrix element kinematic configuration using the MLM algorithm [44], before being processed through a fast simulation of the CMS detector [45]. The SUSY particle production cross sections are calculated to next-to-leading order (NLO) plus next-to-leading-logarithm (NLL) accuracy [46–50], assuming all SUSY particles other than those in the relevant diagram to be too heavy to participate in the interaction. The NLO+NLL cross section and its associated uncertainty [51] are taken as a reference to derive the exclusion limit on the SUSY particle masses.

3 The CMS detector

The central feature of the CMS detector is a superconducting solenoid of 6 m internal diameter, providing a magnetic field of 3.8 T. Within the superconducting solenoid volume are a silicon pixel and a silicon strip tracker, a lead-tungstate crystal electromagnetic calorimeter, and a brass/scintillator hadron calorimeter, each composed of a barrel and two endcap sections. Muons are measured in gas-ionization detectors embedded in the magnet steel flux-return yoke outside the solenoid. Extensive forward calorimetry complements the coverage provided by the barrel and endcap detectors. Jets and leptons are reconstructed within the pseudorapidity region $|\eta| < 3$, covered by the electromagnetic and hadron calorimeters. Muons are reconstructed with $|\eta| < 2.4$. Events are selected by a two-level trigger system. The first level (L1) is based on a hardware filter, followed by a software-based high level trigger (HLT). A more detailed description of the CMS detector, together with a definition of the coordinate system used and the relevant kinematic variables, can be found in Ref. [52].

4 Event selection

Events are selected at the L1 trigger level by requiring at least two jets with $|\eta| < 3$. At the HLT level, events are selected using dedicated razor algorithms, consisting of a loose selection on M_R and R^2 . Razor-specific triggers are used in the HLT in order to avoid biases on the shapes of distributions from the SM background that are introduced by requirements on more traditional selection variables such as E_T^{miss} . The razor triggers reject the majority of the SM background, which mostly appears at low R^2 and low M_R , while retaining events in the signal-sensitive regions of the (M_R , R^2) plane. Two types of triggers are used: i) a hadronic razor trigger, which selects events that contain at least two jets with transverse momentum $p_T > 64 \text{ GeV}$ by applying threshold requirements on R^2 , M_R , and their product; ii) a muon and electron razor trigger, which selects events with at least one isolated electron or muon with $p_T > 12 \text{ GeV}$ in combination with looser requirements on R^2 , M_R , and their product. The trigger efficiency, evaluated using a dedicated trigger, is measured to be $(95 \pm 5)\%$ and is independent of R^2 and M_R for the events selected with the baseline requirements described in Section 5.

Following the trigger selection, events are required to contain at least one reconstructed inter-

action vertex. If more than one vertex is found, the one with the highest p_T^2 sum of associated tracks is chosen as the interaction point for event reconstruction. Algorithms are used to remove events with detector- and beam-related noise that can mimic event topologies with high energy and large p_T imbalance [53–55].

The analysis uses a global event description based on the CMS particle flow (PF) algorithm [56, 57]. Individual particles (PF candidates) are reconstructed by combining the information from the inner tracker, the calorimeters, and the muon system. Five categories of PF candidates are defined: muons, electrons, photons (including their conversions to e^+e^- pairs), charged hadrons, and neutral hadrons. The contamination from other proton-proton collisions in the same or in neighboring bunch crossings is reduced by discarding the charged PF candidates not compatible with the interaction point. When computing lepton isolation and jet energy, the corresponding contamination from neutral particles is subtracted on average by applying an event-by-event correction based on the jet-area method [58–60].

A “tight” lepton identification is used for muons and electrons, consisting of requirements on isolation and track reconstruction quality. For electrons, the shape and position of the energy deposit in the electromagnetic calorimeter is used to further reduce the contamination from hadrons [61]. For events with one identified tight lepton, additional muons or electrons are identified through a “loose” lepton selection, characterized by a relaxed isolation requirement [62]. Tight leptons are required to have $p_T > 15\text{ GeV}$ and loose leptons $p_T > 10\text{ GeV}$.

Jets are reconstructed by clustering the PF candidates with the FASTJET [63] implementation of the anti- k_T [64] algorithm with the distance parameter $R = 0.5$. We select events containing at least two jets with $p_T > 80\text{ GeV}$ and $|\eta| < 2.4$, representing a tighter version of the L1 jet selection criterion. The p_T imbalance in the event, \vec{p}_T^{miss} , is the negative of the sum of the \vec{p}_T of the PF candidates in the event. Its magnitude is referred to as E_T^{miss} . For each event, the \vec{p}_T^{miss} and the four-momenta of all the jets with $p_T > 40\text{ GeV}$ and $|\eta| < 2.4$ are used to compute the razor variables, as described in Section 5.

The medium working point of the combined secondary vertex algorithm [65] is used for b-jet tagging. The b-tagging efficiency and mistag probability are measured from data control samples as a function of the jet p_T and η . Correction factors are derived for Monte Carlo (MC) simulations through comparison of the measured and simulated b-tagging efficiencies and mistag rates found in these control samples [65].

Events with no b-tagged jet are discarded, a criterion motivated by the natural SUSY signatures described in Section 2. A tighter requirement (≥ 2 b-tagged jets) is imposed on events without an identified tight lepton and fewer than four jets. This requirement reduces the expected background from SM production of $Z(\rightarrow \nu\bar{\nu}) + \text{jets}$ events to a negligible level.

5 Box definitions

The selected events are categorized into the different razor boxes according to their event content as shown in Table 1. In the table, the boxes are listed according to the filling order, from the first (at the top of the table) to the last (at the bottom). If an event satisfies the requirements of two or more boxes, the event is assigned to the first listed box to ensure the boxes correspond to disjoint samples.

The events in the single-lepton and two-lepton boxes are recorded using the electron and muon razor trigger. The remaining two boxes, generically referred to as “hadronic” boxes, contain events recorded using the hadronic razor trigger.

In the two-lepton boxes, the (M_R , R^2) distribution of events with at least one b-tagged jet is studied. For the other boxes, the data are binned according to the b-tagged jet multiplicity: 1 b-tag, 2 b-tags, and ≥ 3 b-tags.

Table 1: Kinematic and multiplicity requirements defining the nine razor boxes. Boxes are listed in order of event filling priority.

Box	Lepton	b-tag	Kinematic	Jet
Two-lepton boxes				
MuEle	≥ 1 tight electron and ≥ 1 loose muon			
MuMu	≥ 1 tight muon and ≥ 1 loose muon	≥ 1 b-tag	$(M_R > 300 \text{ GeV and } R^2 > 0.15) \text{ and}$ $(M_R > 350 \text{ GeV or } R^2 > 0.2)$	≥ 2 jets
EleEle	≥ 1 tight electron and ≥ 1 loose electron			
Single-lepton boxes				
MuMultiJet	1 tight muon			
EleMultiJet	1 tight electron	≥ 1 b-tag	$(M_R > 300 \text{ GeV and } R^2 > 0.15) \text{ and}$ $(M_R > 350 \text{ GeV or } R^2 > 0.2)$	≥ 4 jets
MuJet	1 tight muon			
EleJet	1 tight electron			2 or 3 jets
Hadronic boxes				
MultiJet	none	≥ 1 b-tag	$(M_R > 400 \text{ GeV and } R^2 > 0.25) \text{ and}$	≥ 4 jets
≥ 2 b-tagged jet	none	≥ 2 b-tag	$(M_R > 450 \text{ GeV or } R^2 > 0.3)$	2 or 3 jets

A baseline kinematic requirement is applied to define the region in which we search for a signal:

- $M_R > 400 \text{ GeV and } R^2 > 0.25$ for the hadronic boxes;
- $M_R > 300 \text{ GeV and } R^2 > 0.15$ for the other boxes.

The tighter baseline selection for the hadronic boxes is a consequence of the tighter threshold used for the hadronic razor trigger. The kinematic plane defined by the baseline selection is divided into three regions (see Fig. 3):

- Low M_R sideband: $400 < M_R < 550 \text{ GeV and } R^2 > 0.30$ for the hadronic boxes;
 $300 < M_R < 450 \text{ GeV and } R^2 > 0.20$ for the other boxes.
- Low R^2 sideband: $M_R > 450 \text{ GeV and } 0.25 < R^2 < 0.30$ for the hadronic boxes;
 $M_R > 350 \text{ GeV and } 0.15 < R^2 < 0.20$ for the other boxes.
- Signal-sensitive region: $M_R > 550 \text{ GeV and } R^2 > 0.30$ for the hadronic boxes; $M_R > 450 \text{ GeV and } R^2 > 0.20$ for the other boxes.

The bottom left corner of the razor plane, not included in any of the three regions, is excluded from the analysis. Given this selection, the multijet background from quantum chromodynamics processes is reduced to a negligible level due to the fact that these processes typically peak at $R^2 \approx 0$ and fall exponentially for larger values of R^2 [37, 38].

6 Modeling of the standard model backgrounds

Under the hypothesis of no contribution from new-physics processes, the event distribution in the considered portion of the (M_R , R^2) plane can be described by the sum of the contributions from SM V+jets events (where V indicates a W or Z boson) and SM top quark-antiquark and single-top events, where the events with a top quark are generically referred to as the $t\bar{t}$ contribution. Based on MC studies, the contributions from other processes are determined to be negligible.

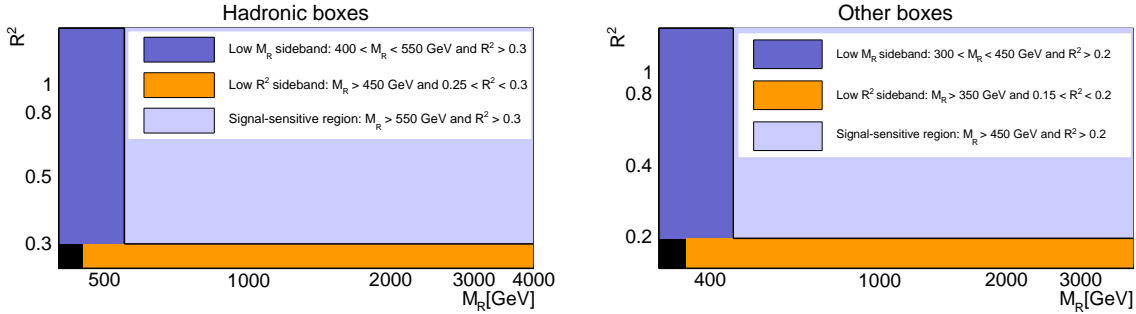


Figure 3: Definition of the sideband and the signal-sensitive regions used in the analysis, for (left) the hadronic boxes and (right) the other boxes.

We study each of these processes using MC samples, generated with the MADGRAPH v5 simulation [42, 43]. Parton shower and hadronization effects are included by matching events to the PYTHIA v6.4.26 simulation [66] using the MLM algorithm [44]. The events are processed by a GEANT-based [67] description of the CMS apparatus in order to account for the response of the detector.

Once normalized to the NLO inclusive cross section and the integrated luminosity, the absolute yield of the V+jets events contribution satisfying the event selection is found to be negligible in all of the two-lepton boxes. In the remaining boxes, its contribution to the total SM background is found to be approximately 25%. The contribution of V+jets events in the ≥ 2 b-tag and the ≥ 4 jet sample is found to be negligible. The remainder of the background in each box originates from $t\bar{t}$ events.

Based on the study of the data collected at $\sqrt{s} = 7$ TeV and the corresponding MC samples [37, 38], the two-dimensional probability density function $P_{SM}(M_R, R^2)$ for each SM process is found to be well described by the empirical function

$$f(M_R, R^2) = [b(M_R - M_R^0)^{1/n}(R^2 - R_0^2)^{1/n} - 1] e^{-bn(M_R - M_R^0)^{1/n}(R^2 - R_0^2)^{1/n}}, \quad (4)$$

where b , n , M_R^0 , and R_0^2 are free parameters of the background model. For $n = 1$, this function recovers the two-dimensional exponential function used for previous studies [37, 38]. The shape of the empirical function is determined through a ROOFIT-based extended and unbinned maximum likelihood fit to the data [68]. Two kinds of fit are performed: (i) a sideband-only fit, which is extrapolated to the signal region in order to test for the presence of a signal (discussed in the remainder of this section), and (ii) a simultaneous fit to the signal and sideband regions, performed both under the background-only and background-plus-signal hypotheses, which is used for the interpretation of the results (Section 7). In both cases, the empirical function is found to adequately describe the SM background in each of the boxes, for each b-tagged jet multiplicity value.

The SM background-only likelihood function for the two-lepton boxes is written as:

$$\mathcal{L}(\text{data}|\Theta) = \frac{e^{-N_{SM}}}{N!} \prod_{i=1}^N N_{SM} P_{SM}(M_{R(i)}, R^2_{(i)}), \quad (5)$$

where $P_{SM}(M_R, R^2)$ is the empirical function in Eq. (4) normalized to unity, N_{SM} is the corresponding normalization factor, Θ is the set of background shape and normalization parameters, and the product runs over the N events in the data set. The same form of the likelihood is used for the other boxes, for each b-tagged jet multiplicity. The total likelihood in these boxes is computed as the product of the likelihood functions for each b-tagged jet multiplicity.

The fits are performed independently for each box and simultaneously across the b-tagged jet multiplicity bins. Common background shape parameters (b , M_R^0 , R_0^2 , and n) are used for the 2 b-tag and ≥ 3 b-tag bins, since no substantial difference between the two distributions is observed on large samples of $t\bar{t}$ and V+jets MC events. A difference is observed between 1 b-tag and ≥ 2 b-tag samples, due to the observed dependence of the b-tagging efficiency on the jet p_T . Consequently, the shape parameters for the 1 b-tag bins are allowed to differ from the corresponding parameters for the ≥ 2 b-tag bins. The background normalization parameters for each b-tagged jet multiplicity bin are also treated as independent parameters.

The background shape parameters are estimated from the events in the two sidebands (Section 5). This shape is then used to derive a background prediction in the signal-sensitive region: 30 000 alternative sets of background shape parameters are generated from the covariance matrix returned by the fit. An ensemble of pseudo-experiment data sets is created, generating random (M_R , R^2) pairs distributed according to each of these alternative shapes. For each bin of the signal-sensitive region, the distribution of the predicted yields in each pseudo-experiment is compared to the observed yield in data in order to quantify the agreement between the background model and the observation. The agreement, described as a two-sided p-value, is then translated into the corresponding number of standard deviations for a normal distribution. The p-value is computed using the probability density as the ordering principle. The observed numbers of standard deviations in the two-lepton boxes are shown in Fig. 4, as a function of M_R and R^2 . Positive and negative significance correspond to regions where the observed yield is respectively larger and smaller than the predicted one. Light gray areas correspond to empty bins with less than one event expected on average. Similar results for the one-lepton and hadronic boxes are shown in Figs. 5 and 6. Figures 7–10 illustrate the extrapolation of the fit results to the full (M_R , R^2) plane, projected onto R^2 and M_R and summed over the b-tagged jet multiplicity bins. No significant deviation of data from the SM background predictions is observed.

To demonstrate the discovery potential of this analysis, we apply the background-prediction procedure to a simulated signal-plus-background MC sample. Figure 11 shows the M_R and R^2 distributions of SM background events and T1bbbb events (Section 2). The gluino and LSP masses are set respectively to 1325 GeV and 50 GeV, representing a new-physics scenario near the expected sensitivity of the analysis. A signal-plus-background sample is obtained by adding the two distributions of Fig. 11, assuming an integrated luminosity of 19.3 fb^{-1} and a gluino-gluino production cross section of 0.02 pb, corresponding to 78 expected signal events in the signal-sensitive region. The agreement between the background prediction from the sideband fit and the yield of the signal-plus-background pseudo-experiments is displayed in Fig. 12. The contribution of signal events to the sideband region has a negligible impact on the determination of the background shape, while a disagreement is observed in the signal-sensitive region, characterized as an excess of events clustered around $M_R \approx 1300 \text{ GeV}$. The excess indicates the presence of a signal, and the position of the excess in the M_R variable provides information about the underlying SUSY mass spectrum.

7 Limit-setting procedure

We interpret the results of the searches by determining the 95% confidence level (CL) upper limits on the production cross sections of the SUSY models presented in Section 2, using the LHC CL_s procedure [40] and a global likelihood determined by combining the likelihoods of the different search boxes and sidebands. To reduce computational requirements, a binned likelihood is used.

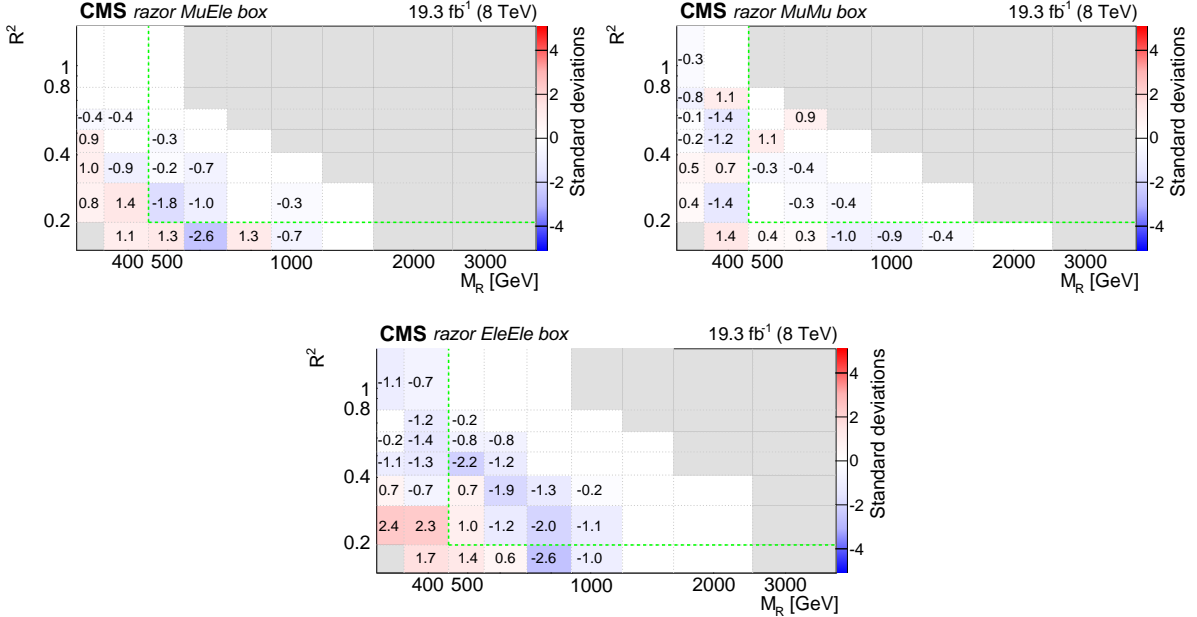


Figure 4: Comparison of the expected background and the observed yield in the (upper left) MuEle, (upper right) MuMu, and (bottom) EleEle boxes. A probability density function is derived for the bin-by-bin yield using pseudo-experiments, sampled from the output of the corresponding sideband fit. A two sided p-value is computed comparing the observed yield to the distribution of background yield from pseudo-experiments. The p-value is translated into the corresponding number of standard deviations, quoted in each bin and represented by the bin-filling color. Positive and negative significance correspond to regions where the observed yield is respectively larger and smaller than the predicted one. The white areas correspond to bins in which a difference smaller than 0.1 standard deviations is observed. The gray areas correspond to empty bins with less than one background event expected on average. The dashed lines represent the boundaries between the sideband and the signal regions.

For the razor search boxes, the signal contribution is modeled by a template function, for a given signal hypothesis in a specific box and a given b-tagged jet multiplicity. The template function, normalized to unit probability, is multiplied by the expected signal yield in each bin ($\sigma_{\text{NLO+NLL}} L \epsilon_{\text{b-tag}}^{\text{box}}$). Here $\sigma_{\text{NLO+NLL}}$ is the SUSY signal cross section, L is the integrated luminosity corresponding to the size of the data set, and $\epsilon_{\text{b-tag}}^{\text{box}}$ is the signal selection efficiency for a given box and, in case of the single-lepton and hadronic boxes, for a given b-tagged jet multiplicity.

Each systematic uncertainty is incorporated in the likelihood with a dedicated nuisance parameter, whose value is not known a priori but rather must be estimated from the data. The set of nuisance parameters may be divided into three distinct classes (though their statistical treatment is the same): those related to the signal normalization, those related to the signal shape, and those related to the background normalization and shape.

We consider the following systematic uncertainties associated with the signal normalization, with the size of the uncertainty indicated in parentheses:

- integrated luminosity (2.6%) [69];
- trigger efficiency (5%);
- lepton reconstruction and identification efficiencies (3% per lepton), measured from

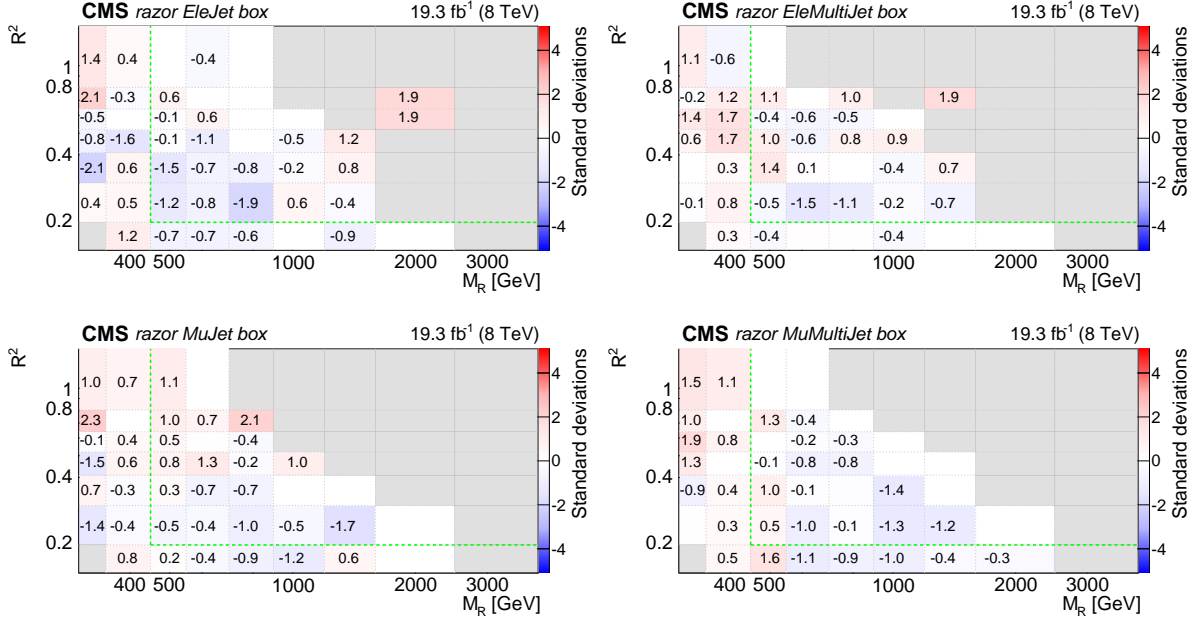


Figure 5: Comparison of the expected background and the observed yield in (upper left) the EleJet, (upper right) the EleMultiJet, (lower left) the MuJet, and (lower right) the MuMultiJet boxes. A detailed explanation is given in the caption of Fig. 4.

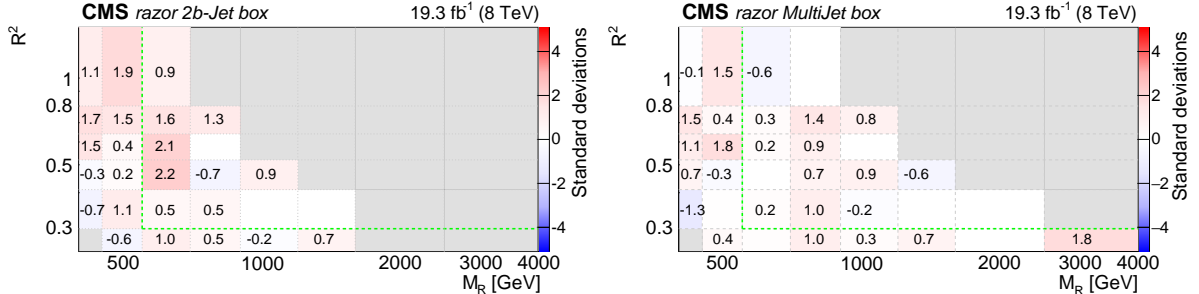


Figure 6: Comparison of the expected background and the observed yield in the ≥ 2 b-tagged jet box (left) and the MultiJet box (right). A detailed explanation is given in the caption of Fig. 4.

an inclusive $Z \rightarrow \ell^+ \ell^-$ event sample ($\ell = e, \mu$) as a function of the lepton p_T and η values [61, 62].

In addition, four signal-shape systematic uncertainties are considered, whose sizes vary with R^2 , M_R , and the b-tagged jet multiplicity:

- The uncertainty in the jet b-tagging and mistagging efficiencies (up to 20% depending on the signal model), evaluated for each (M_R, R^2) and b-tagged jet multiplicity bin. The uncertainty is evaluated by propagating the uncertainty in data-to-simulation scale factors [65].
- the uncertainty in the modeling of the parton distribution functions (PDFs) (up to 10% depending on the signal model), evaluated for each bin in the (M_R, R^2) plane and for each box and b-tag multiplicity following the PDF4LHC [70–72] prescription, using the CTEQ-6.6 [73] and MRST-2006-NNLO [74] PDF sets.
- The uncertainty in the jet energy scale and resolution (up to 5% depending on the signal model), evaluated from a set of data control samples and MC simulations [60].

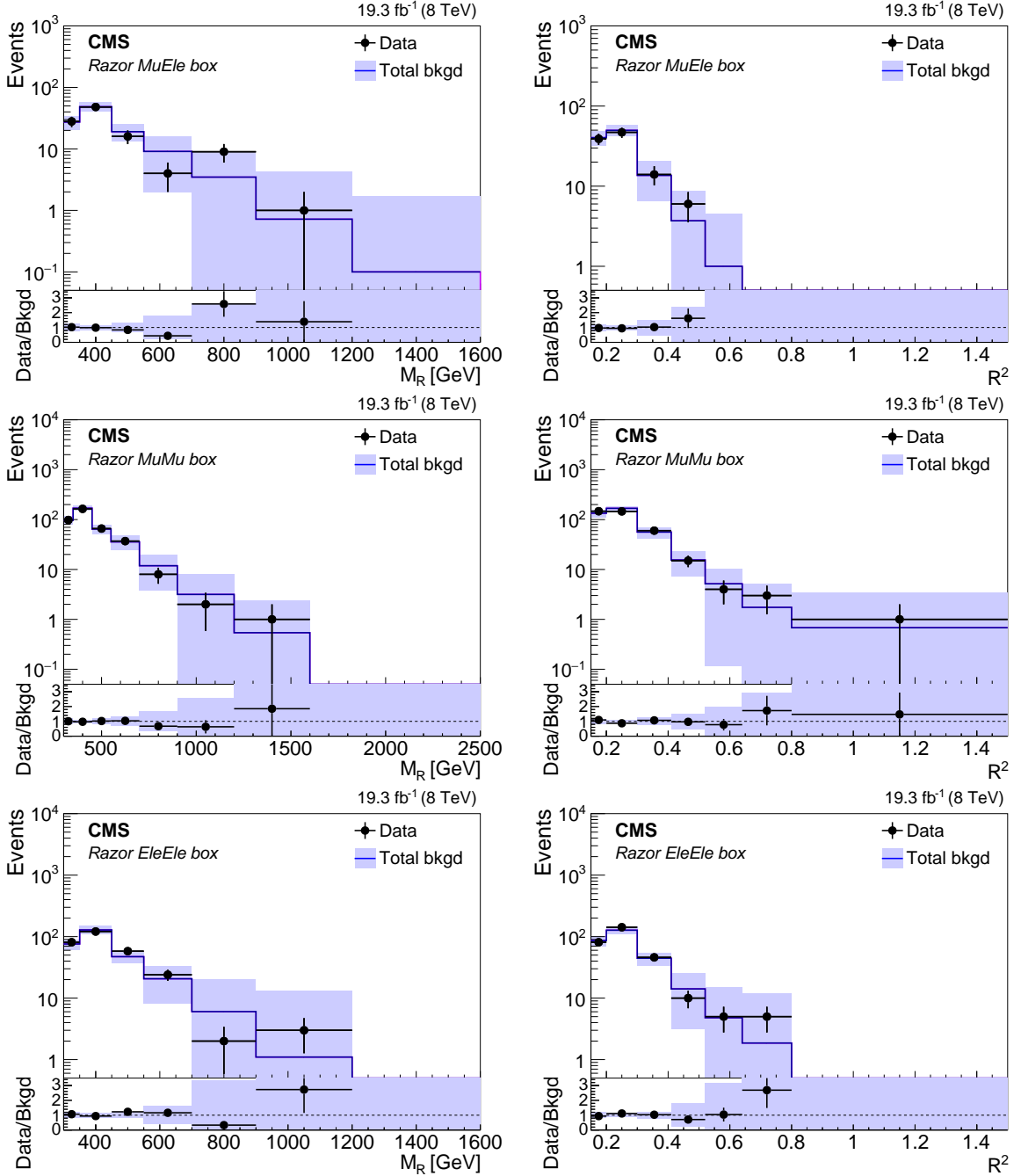


Figure 7: Projection of the sideband fit result in the (upper row) MuEle, (middle row) MuMu, and (lower row) EleEle boxes on M_R (left) and R^2 (right), respectively. The fit is performed in the sideband regions and extrapolated to the signal-sensitive region. The solid line and the filled band represent the total background prediction and its uncertainty. The points and the band in the bottom panel represent the data-to-prediction ratio and the prediction uncertainty, respectively.

- The uncertainty in the modeling of the associated jet production by the MADGRAPH simulation (up to 20% depending on the signal model), studied using Z+jets and $t\bar{t}$ data events and parameterized by an MC-to-data scale factor as a function of the magnitude of the vector sum of the p_T values of the two produced SUSY particles [19].

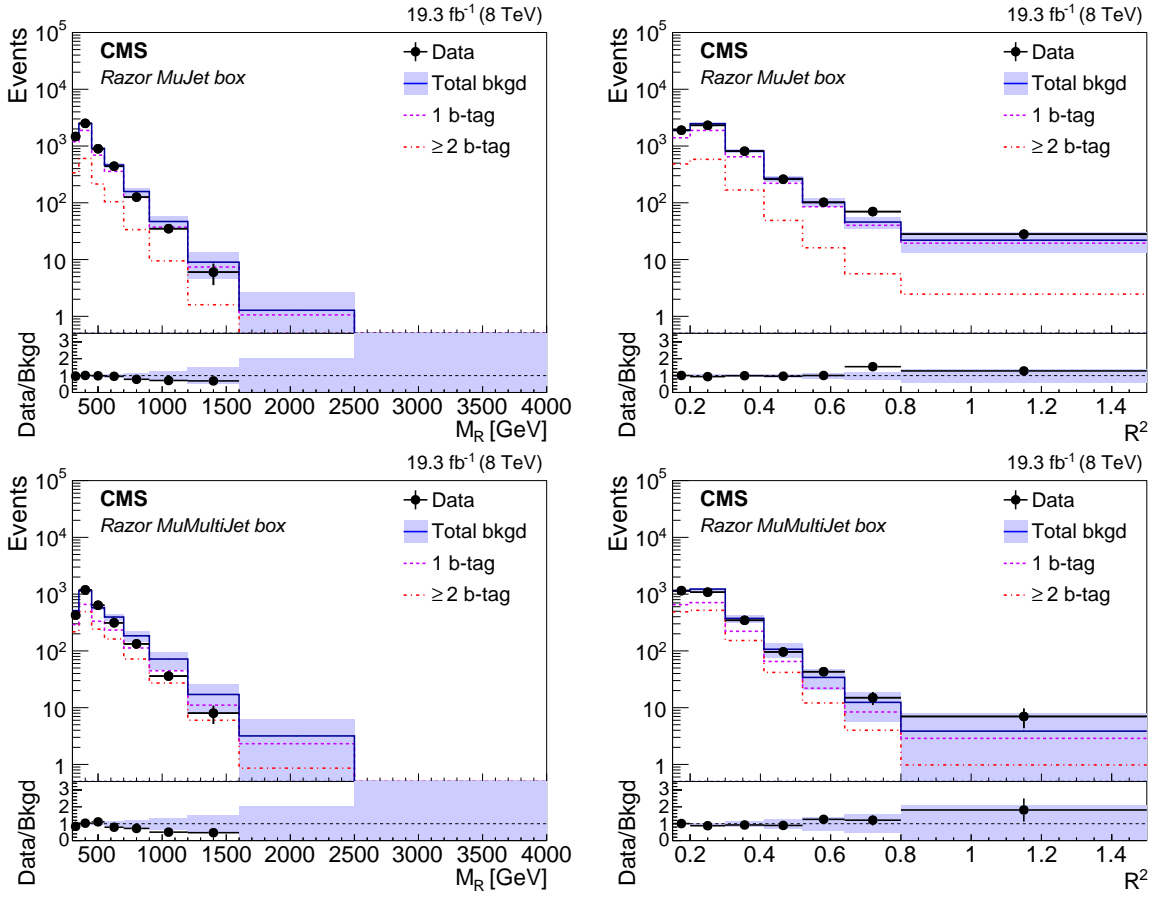


Figure 8: Projection of the sideband fit result in the MuJet box on (upper left) M_R and (upper right) R^2 , and of the sideband fit result in the MuMultiJet box on (lower left) M_R and (lower right) R^2 . The fit is performed in the sideband regions and extrapolated to the signal-sensitive region. The solid line and the filled band represent the total background prediction and its uncertainty. The dashed and dot-dashed lines represent the background shape for 1 b-tag and ≥ 2 b-tag events, respectively. The points and the band in the bottom panel represent the data-to-prediction ratio and the prediction uncertainty, respectively.

The impact of each of these uncertainties on the SUSY signal shape is taken into account by varying each effect up or down by one standard deviation.

The uncertainty in the knowledge of the background distributions is taken into account by maximizing the likelihood with respect to the background shape and normalization parameters using the data in the two sidebands and the signal-sensitive region. The background parameterization is able to accommodate several sources of systematic uncertainties defined below:

- dependence of the background shape on the b-tag multiplicity;
- dependence of the background shape on the lepton and jet multiplicities;
- deviation of the two-dimensional shape from an exponentially falling distribution, through the background empirical function parameter n , which modifies the tail in M_R and R^2 ;
- shape bias induced by the dependence of the b-tagging efficiency and mistag rate on the jet p_T ;

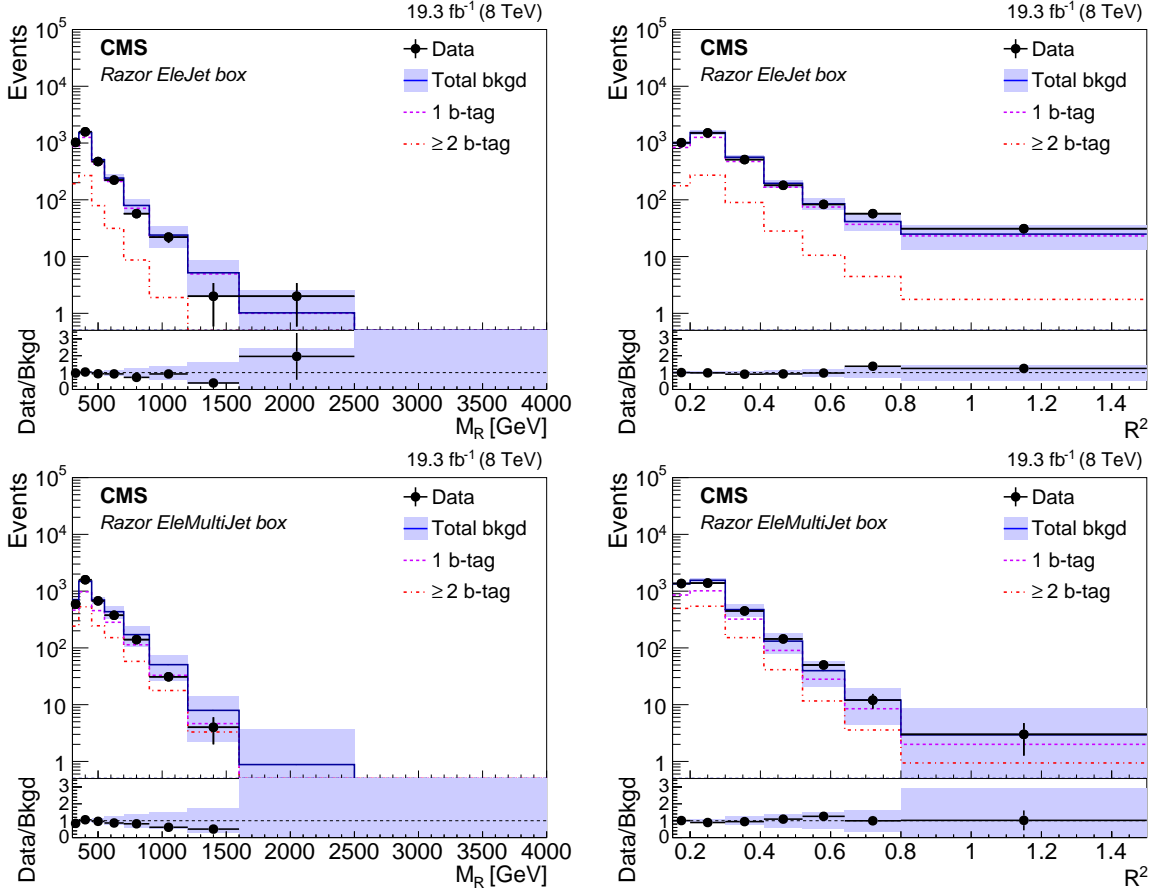


Figure 9: Projection of the sideband fit result in the EleJet box on (upper left) M_R and (upper right) R^2 , and projection of the sideband fit result in the EleMultiJet box on (lower left) M_R and (lower right) R^2 . A detailed explanation is given in the caption of Fig. 8.

- deviation of the b-tagging and mistagging efficiencies from the MC prediction, through independent normalization factors in each b-tagged jet multiplicity bin.

The combination of razor and exclusive single-lepton [19] searches is performed using the same procedure, taking into account the systematic uncertainties associated with the five following effects:

- the PDFs;
- the jet energy scale correction;
- the integrated luminosity;
- the b-jet tagging efficiency;
- the associated jet production.

The uncertainties in the background predictions are taken to be uncorrelated, being derived from independent data control samples with different techniques. We verified that the correlation model for the systematics has a negligible impact on the combination, since similar results are obtained when neglecting any correlation between the systematic uncertainties of the two searches.

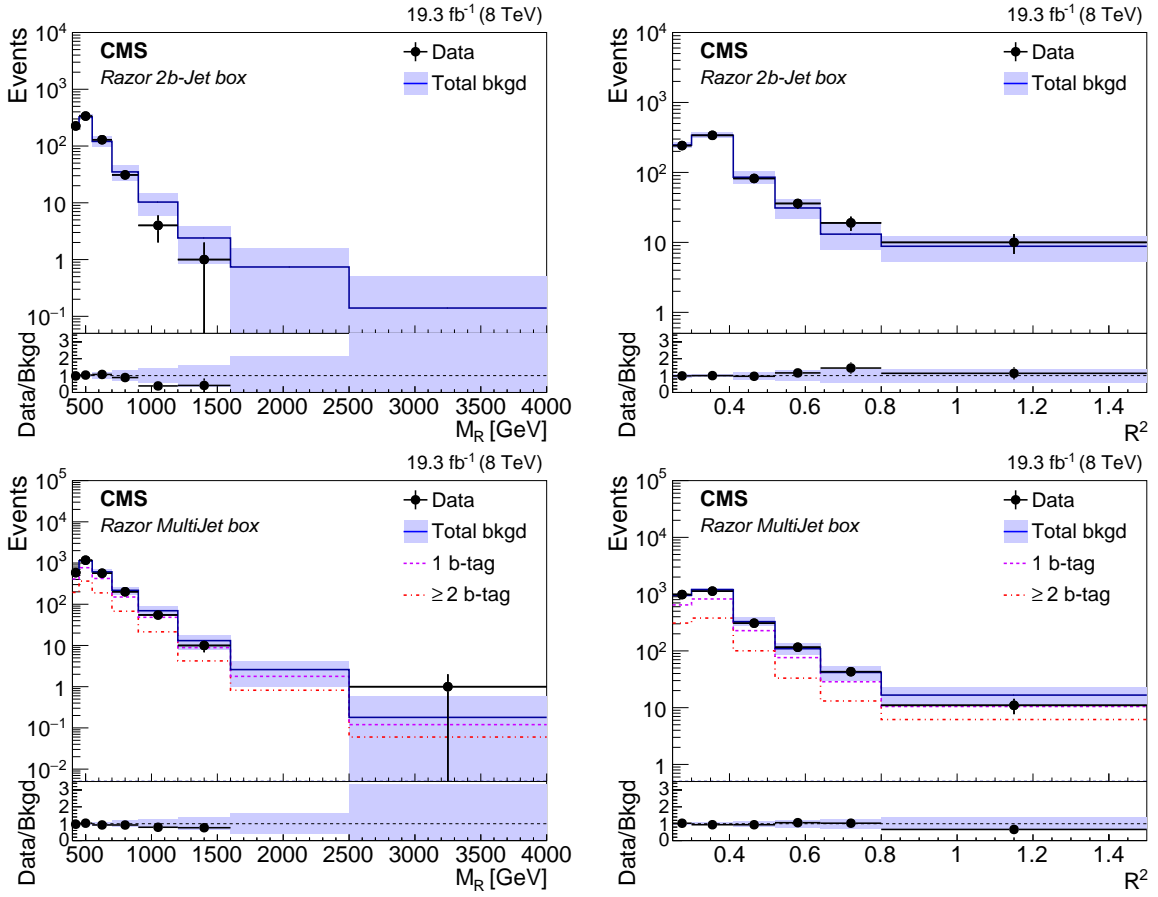


Figure 10: Projection of the sideband fit result in the ≥ 2 b-tagged jet box on (upper left) M_R and (upper right) R^2 , and projection of the sideband fit result in the MultiJet box on (lower left) M_R and (lower right) R^2 . A detailed explanation is given in the caption of Fig. 8.

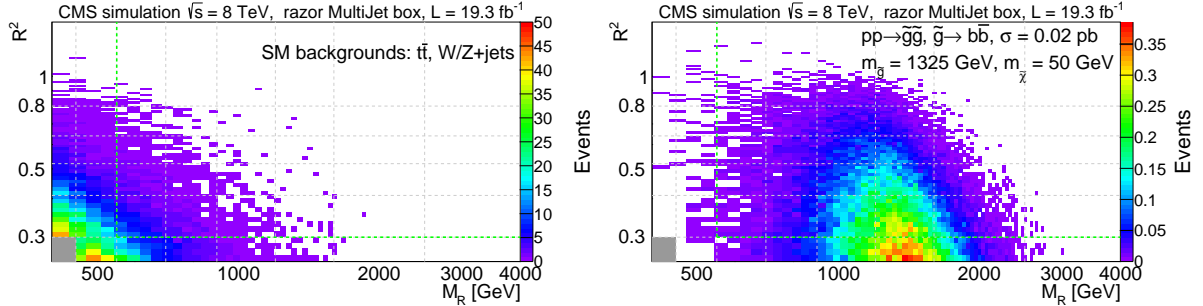


Figure 11: Distribution of (left) simulated SM background events and (right) T1bbbb gluino-gluino events in the MultiJet box. Each \tilde{g} is forced to decay to a $b\bar{b}$ pair and a $\tilde{\chi}_1^0$, assumed to be the stable LSP. The \tilde{g} and $\tilde{\chi}_1^0$ masses are fixed to 1325 GeV and 50 GeV, respectively.

8 Interpretation

The results of this search are interpreted in the context of the natural SUSY simplified models presented in Section 2.

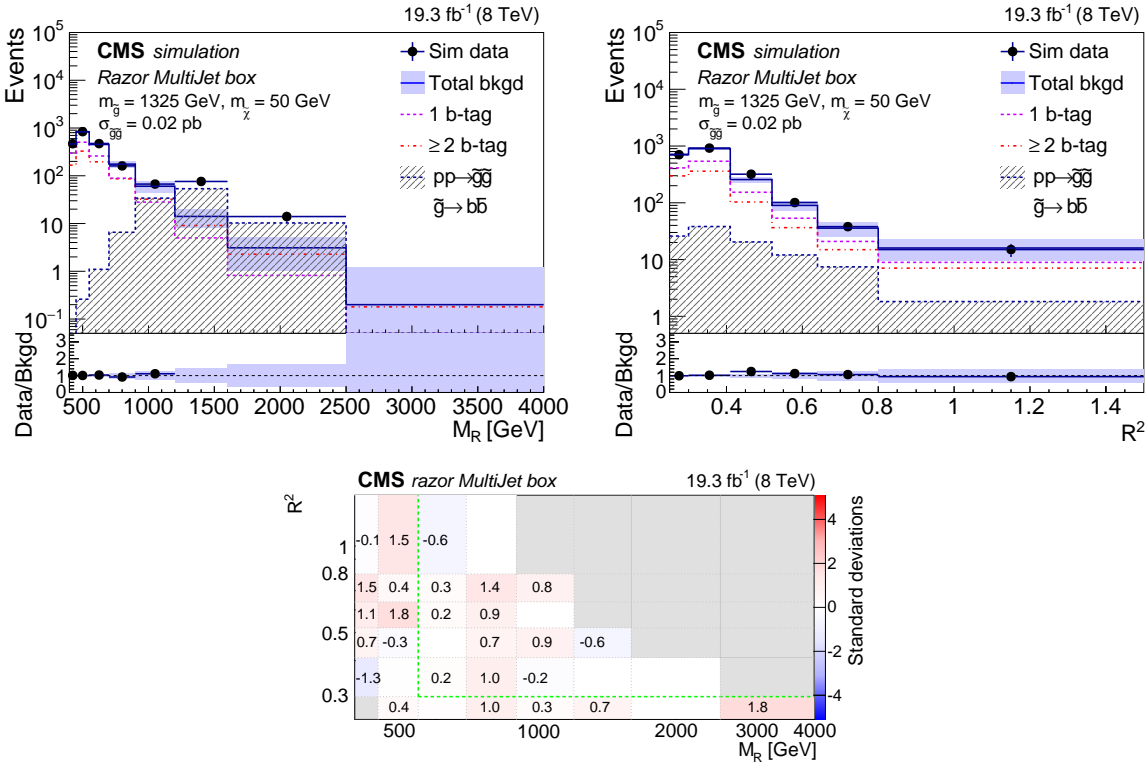


Figure 12: Result of the fit to the sideband events of a signal-plus-background MC sample, corresponding to the gluino model whose distribution is shown in Fig. 11. A gluino-gluino production cross section of 0.02 pb is assumed. The one-dimensional projections on (upper left) M_R and (upper right) R^2 are shown, together with (bottom) the agreement between the observed yield and the prediction from the sideband fit as a function of R^2 and M_R . This agreement is evaluated from a two-sided p-value using an ensemble of background-only pseudo-experiments as described in Section 6.

8.1 Limits on gluino pair production

Derived limits on gluino pair production in the T1bbbb, T1tbbb, T1ttbb, T1tttb, and T1tttt scenarios are presented in Fig. 13. A comparison of the simplified natural SUSY gluino-gluino exclusions, obtained for the different decay-mode combinations of third generation quarks, is shown in Fig. 14. The limits corresponding to gluino-gluino topologies with mixed branching fractions lie within the band defined by the T1bbbb and the T1tttt contours. As an example, gluino masses smaller than 1175 GeV for T1tttt and 1310 GeV for T1bbbb are excluded, for an LSP mass of 100 GeV. For any LSP mass value, a larger number of top quarks in the decay topology corresponds to a weaker limit, mainly due to a reduced total signal efficiency with respect to the four-bottom-quark final state and a worse M_R and R^2 resolution for events with higher jet multiplicity in the final state. Given this fact and the inclusive nature of the analysis, the T1tttt limit can be considered to represent a conservative estimate of a branching-fraction-independent limit, generically valid for gluino-gluino production within the context of the natural SUSY spectrum shown in Fig. 1.

8.2 Limits on top-squark pair production

Derived limits on squark pair production from the razor variables in the T2bW*, T2tb, and T2tt scenarios are presented in Fig. 15 and compared in Fig. 16. As in the case of the gluino interpretation, the expected limit from the razor search improves as the number of top quarks

in the decay topology decreases. For an LSP mass of 100 GeV, top-squark mass values larger than 400 GeV and smaller than 650 GeV are excluded in all three top-squark branching fraction scenarios.

Within the considered scenarios, a top-squark decay to a chargino (neutralino) is topologically similar to a bottom-squark decay to a neutralino (chargino). In the limit of degenerate charginos and neutralinos, the decay products of the chargino are generically too soft to be detected and this correspondence is exact. However, for large mass differences between the squarks and the chargino, the chargino decay products may be boosted enough to become observable, breaking the correspondence. For the models with the intermediate decay to charginos, there is a migration of reconstructed events from the low-background 2b-Jet box to the high-background MultiJet box and a consequently weaker limit with respect to the simplified model without decays to charginos.

A stronger limit on top-squark pair production is derived by combining the hadronic boxes of the razor search with the results of the exclusive single-lepton analysis [19]. The exclusive single-lepton search is conservatively assumed to only have sensitivity when both top squarks decay to a top quark and a neutralino. Figure 17 (left) presents the combined result obtained for the scenario where the top squark only decays to a top quark and the lightest neutralino. For an LSP mass of 100 GeV, the combination improves the constraint on the top-squark mass from 660 to 730 GeV. This result provides the most stringent limit on this specific simplified model.

Figure 17 (right) presents a more generic limit on the top-squark mass. We consider two decay modes for the top squark, as indicated in Fig. 1. We scan the relative branching fractions, assuming that no other decay mode is allowed. The largest excluded cross section (that is, the worst upper limit) is found for each choice of the top-squark and neutralino mass. A branching-fraction-independent limit is derived by comparing the worst-case exclusion to the corresponding top-squark pair production cross section. In this manner, top squarks decaying to the two considered decay modes are excluded at a 95% confidence level for mass values >400 GeV and <645 GeV, assuming a neutralino mass of 100 GeV. Unlike other simplified model interpretations, this interpretation is not based on a specific choice of branching fractions. While a residual model dependence is present because only two decay modes are considered, this result is more general than previous constraints.

9 Summary

We present a search for supersymmetric particles using proton-proton collision data collected by CMS in 2012 at $\sqrt{s} = 8$ TeV. The data set size corresponds to an integrated luminosity of 19.3 fb^{-1} . We consider events with at least two jets, at least one of which is identified as a b-tagged jet, and study the event distribution in the razor variables (M_R , R^2). The data are classified according to the muon, electron, jet, and b-tagged jet multiplicities. No significant excess is observed with respect to the standard model background expectations, derived from a fit to the data distribution in low- M_R and low- R^2 sidebands.

The inclusive razor search is translated into 95% confidence level exclusion limits on the masses of the gluino and the top squark, in the context of simplified “natural” SUSY models. For a neutralino mass of 100 GeV and depending on the branching fractions, the pair production of gluinos and top squarks in multi-bottom, multi-top, and mixed top-plus-bottom quark topologies is excluded for gluino masses up to 1310 GeV and top-squark masses up to 660 GeV. Using the combined likelihood of the hadronic boxes of the razor search and the single-lepton chan-

nels of the exclusive top-squark search [19], the exclusion bound on the top-squark mass is extended to 730 GeV for a top squark decaying to a top quark and to a neutralino of mass 100 GeV. Again assuming the neutralino mass to be 100 GeV, top squarks decaying to the two considered decay modes are excluded at a 95% confidence level for mass values between 400 and 645 GeV, independent of the branching fractions.

Acknowledgments

We congratulate our colleagues in the CERN accelerator departments for the excellent performance of the LHC and thank the technical and administrative staffs at CERN and at other CMS institutes for their contributions to the success of the CMS effort. In addition, we gratefully acknowledge the computing centers and personnel of the Worldwide LHC Computing Grid for delivering so effectively the computing infrastructure essential to our analyses. Finally, we acknowledge the enduring support for the construction and operation of the LHC and the CMS detector provided by the following funding agencies: the Austrian Federal Ministry of Science, Research and Economy and the Austrian Science Fund; the Belgian Fonds de la Recherche Scientifique, and Fonds voor Wetenschappelijk Onderzoek; the Brazilian Funding Agencies (CNPq, CAPES, FAPERJ, and FAPESP); the Bulgarian Ministry of Education and Science; CERN; the Chinese Academy of Sciences, Ministry of Science and Technology, and National Natural Science Foundation of China; the Colombian Funding Agency (COLCIENCIAS); the Croatian Ministry of Science, Education and Sport, and the Croatian Science Foundation; the Research Promotion Foundation, Cyprus; the Ministry of Education and Research, Estonian Research Council via IUT23-4 and IUT23-6 and European Regional Development Fund, Estonia; the Academy of Finland, Finnish Ministry of Education and Culture, and Helsinki Institute of Physics; the Institut National de Physique Nucléaire et de Physique des Particules / CNRS, and Commissariat à l’Énergie Atomique et aux Énergies Alternatives / CEA, France; the Bundesministerium für Bildung und Forschung, Deutsche Forschungsgemeinschaft, and Helmholtz-Gemeinschaft Deutscher Forschungszentren, Germany; the General Secretariat for Research and Technology, Greece; the National Scientific Research Foundation, and National Innovation Office, Hungary; the Department of Atomic Energy and the Department of Science and Technology, India; the Institute for Studies in Theoretical Physics and Mathematics, Iran; the Science Foundation, Ireland; the Istituto Nazionale di Fisica Nucleare, Italy; the Ministry of Science, ICT and Future Planning, and National Research Foundation (NRF), Republic of Korea; the Lithuanian Academy of Sciences; the Ministry of Education, and University of Malaya (Malaysia); the Mexican Funding Agencies (CINVESTAV, CONACYT, SEP, and UASLP-FAI); the Ministry of Business, Innovation and Employment, New Zealand; the Pakistan Atomic Energy Commission; the Ministry of Science and Higher Education and the National Science Centre, Poland; the Fundação para a Ciência e a Tecnologia, Portugal; JINR, Dubna; the Ministry of Education and Science of the Russian Federation, the Federal Agency of Atomic Energy of the Russian Federation, Russian Academy of Sciences, and the Russian Foundation for Basic Research; the Ministry of Education, Science and Technological Development of Serbia; the Secretaría de Estado de Investigación, Desarrollo e Innovación and Programa Consolider-Ingenio 2010, Spain; the Swiss Funding Agencies (ETH Board, ETH Zurich, PSI, SNF, UniZH, Canton Zurich, and SER); the Ministry of Science and Technology, Taipei; the Thailand Center of Excellence in Physics, the Institute for the Promotion of Teaching Science and Technology of Thailand, Special Task Force for Activating Research and the National Science and Technology Development Agency of Thailand; the Scientific and Technical Research Council of Turkey, and Turkish Atomic Energy Authority; the National Academy of Sciences of Ukraine, and State Fund for Fundamental Researches, Ukraine; the Science and Technology

Facilities Council, UK; the US Department of Energy, and the US National Science Foundation.

Individuals have received support from the Marie-Curie program and the European Research Council and EPLANET (European Union); the Leventis Foundation; the A. P. Sloan Foundation; the Alexander von Humboldt Foundation; the Belgian Federal Science Policy Office; the Fonds pour la Formation à la Recherche dans l'Industrie et dans l'Agriculture (FRIA-Belgium); the Agentschap voor Innovatie door Wetenschap en Technologie (IWT-Belgium); the Ministry of Education, Youth and Sports (MEYS) of the Czech Republic; the Council of Science and Industrial Research, India; the HOMING PLUS program of Foundation for Polish Science, co-financed from European Union, Regional Development Fund; the Compagnia di San Paolo (Torino); the Consorzio per la Fisica (Trieste); MIUR project 20108T4XTM (Italy); the Thalis and Aristeia programs cofinanced by EU-ESF and the Greek NSRF; and the National Priorities Research Program by Qatar National Research Fund.

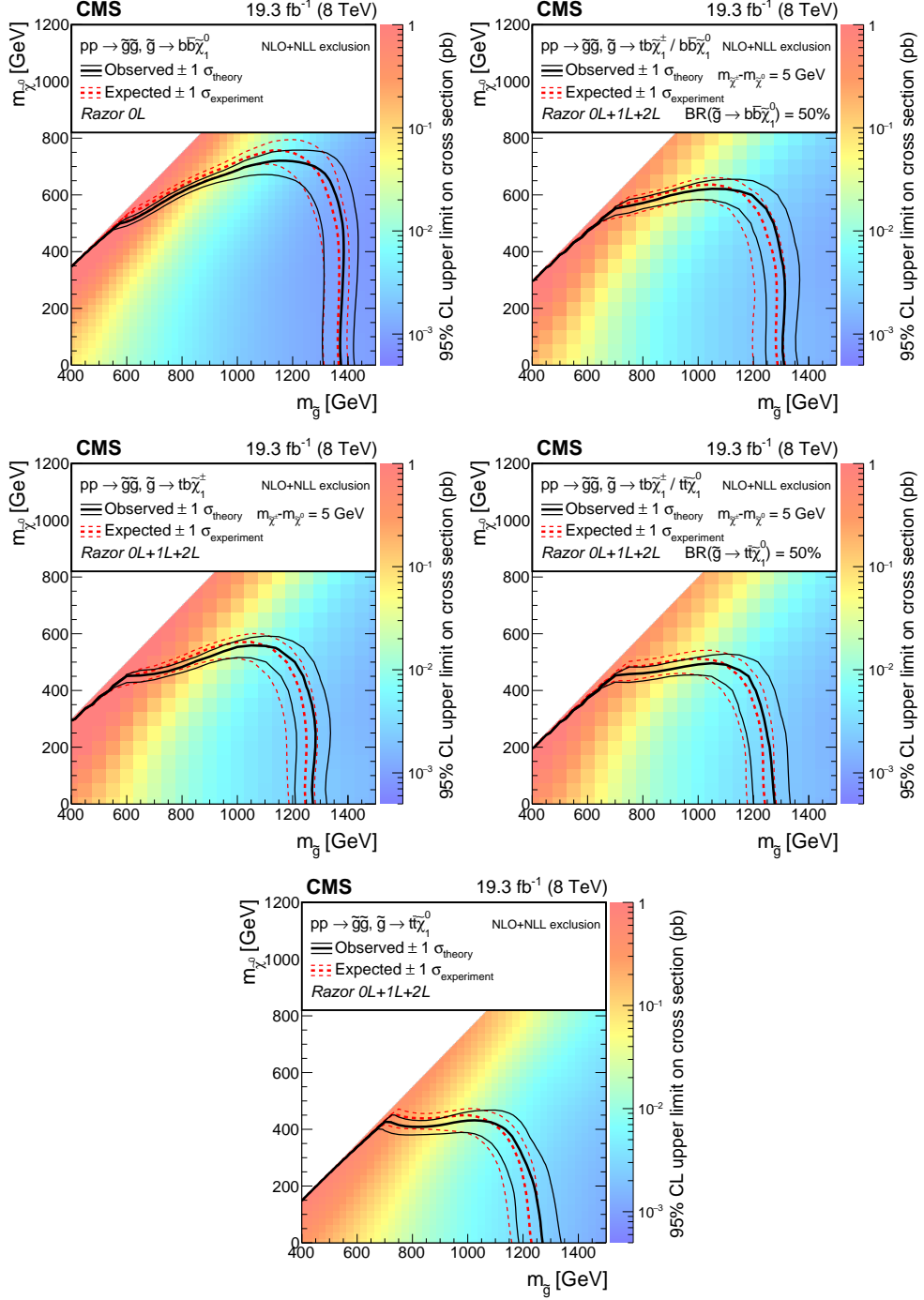


Figure 13: Interpretation of the inclusive search with razor variables in the context of gluino pair production models: (upper left) T1bbbb, (upper right) T1tbbb, (middle left) T1ttbb, (middle right) T1tttb, and (bottom) T1tttt. The limit for T1bbbb is derived using only the hadronic boxes, while the limits for the remaining models are derived using all nine boxes. The color coding indicates the observed 95% CL upper limit on the signal cross section. The dashed and solid lines represent the expected and observed exclusion contours at a 95% CL, respectively. The dashed contours around the expected limit and the solid contours around the observed one represent the one standard deviation theoretical uncertainties in the cross section and the combination of the statistical and experimental systematic uncertainties, respectively.

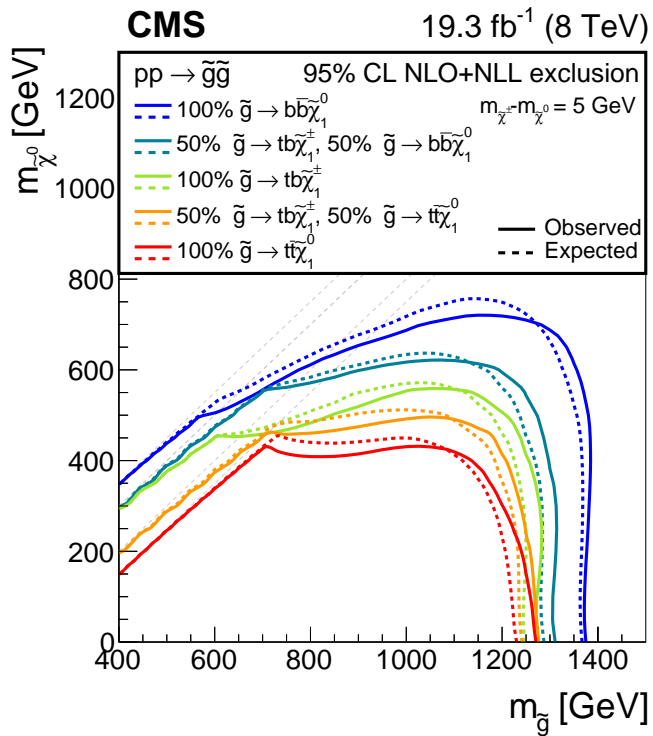


Figure 14: Gluino mass limit at a 95% CL, obtained for different gluino pair production models with the inclusive razor analysis in the context of the natural SUSY spectrum of Fig. 1.

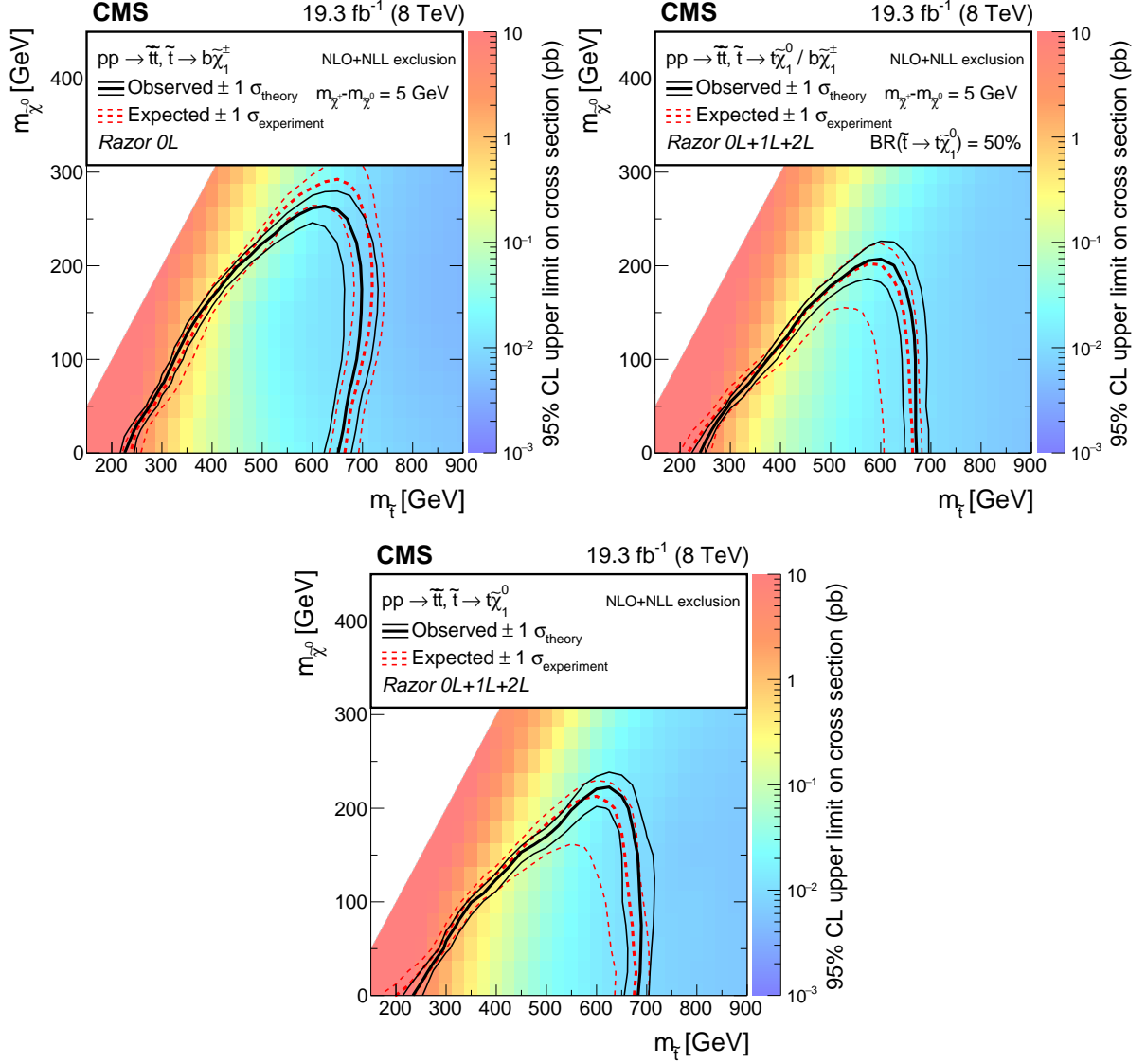


Figure 15: Interpretation of the inclusive search with razor variables in the context of top-squark pair production models: (upper left) T2bW*, (upper right) T2tb, and (bottom) T2tt. The limit for T2bW* is derived using only the hadronic boxes, while the limits for the remaining models are derived using all nine boxes. The meaning of the color coding and the displayed contours is explained in the caption of Fig. 13.

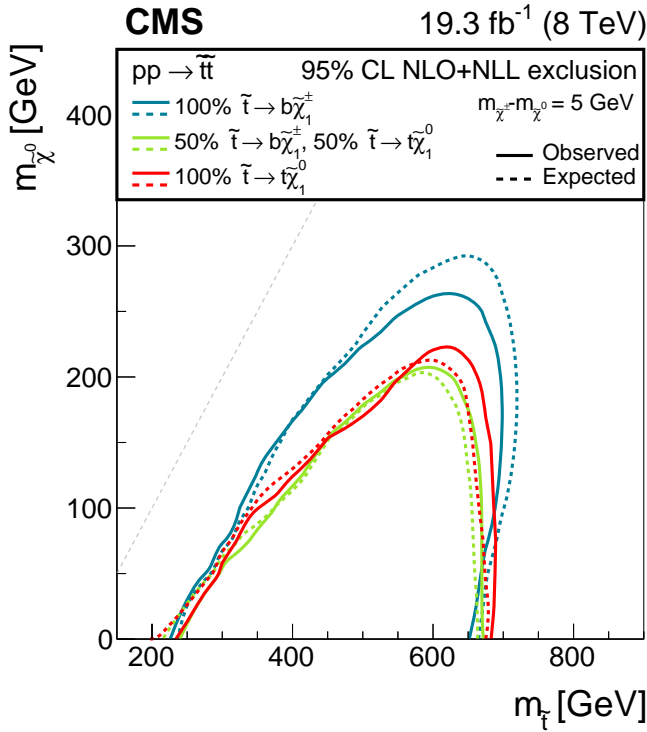


Figure 16: Top-squark mass limit at a 95% CL, obtained for different squark pair production models with the inclusive razor analysis in the context of the natural SUSY spectrum of Fig. 1.

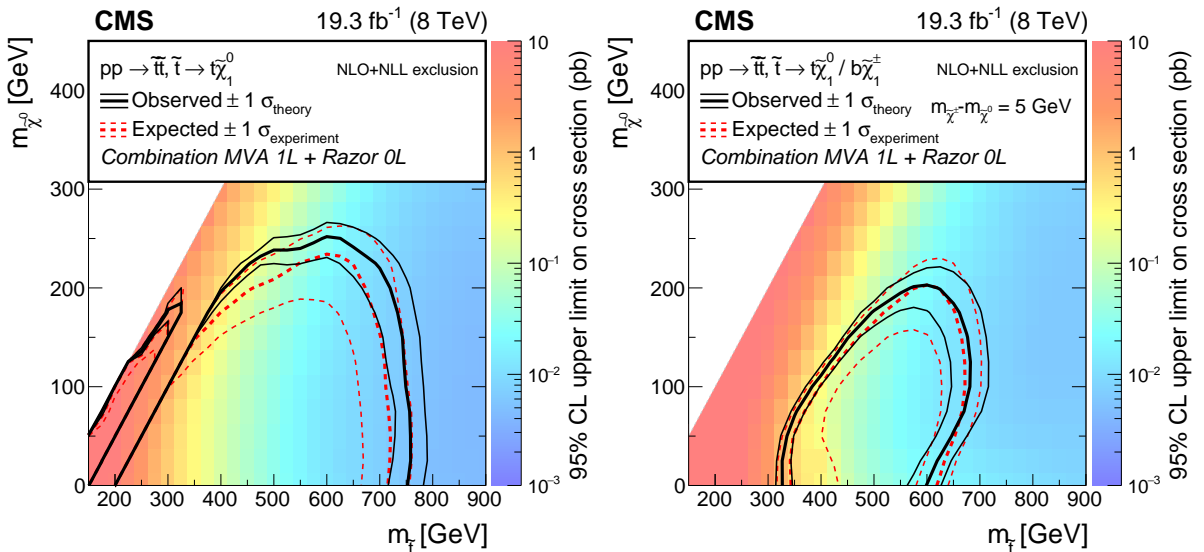


Figure 17: Top-squark mass limit at a 95% CL, obtained combining the result of the hadronic razor boxes with the result of Ref. [19] for (left) T2tt and (right) independent of the branching fraction choice. The meaning of the color coding and the displayed contours is explained in the caption of Fig. 13.

References

- [1] J. Wess and B. Zumino, “Supergauge transformations in four-dimensions”, *Nucl. Phys. B* **70** (1974) 39, doi:10.1016/0550-3213(74)90355-1.
- [2] Y. A. Gol’fand and E. P. Likhtman, “Extension of the algebra of Poincare group generators and violation of P invariance”, *JETP Lett.* **13** (1971) 323.
- [3] D. V. Volkov and V. P. Akulov, “Possible universal neutrino interaction”, *JETP Lett.* **16** (1972) 438.
- [4] A. H. Chamseddine, R. L. Arnowitt, and P. Nath, “Locally supersymmetric grand unification”, *Phys. Rev. Lett.* **49** (1982) 970, doi:10.1103/PhysRevLett.49.970.
- [5] G. L. Kane, C. F. Kolda, L. Roszkowski, and J. D. Wells, “Study of constrained minimal supersymmetry”, *Phys. Rev. D* **49** (1994) 6173, doi:10.1103/PhysRevD.49.6173, arXiv:hep-ph/9312272.
- [6] P. Fayet, “Supergauge invariant extension of the Higgs mechanism and a model for the electron and its neutrino”, *Nucl. Phys. B* **90** (1975) 104, doi:10.1016/0550-3213(75)90636-7.
- [7] R. Barbieri, S. Ferrara, and C. A. Savoy, “Gauge models with spontaneously broken local supersymmetry”, *Phys. Lett. B* **119** (1982) 343, doi:10.1016/0370-2693(82)90685-2.
- [8] L. J. Hall, J. D. Lykken, and S. Weinberg, “Supergravity as the messenger of supersymmetry breaking”, *Phys. Rev. D* **27** (1983) 2359, doi:10.1103/PhysRevD.27.2359.
- [9] P. Ramond, “Dual theory for free fermions”, *Phys. Rev. D* **3** (1971) 2415, doi:10.1103/PhysRevD.3.2415.
- [10] ATLAS Collaboration, “Observation of a new particle in the search for the Standard Model Higgs boson with the ATLAS detector at the LHC”, *Phys. Lett. B* **716** (2012) 1, doi:10.1016/j.physletb.2012.08.020, arXiv:1207.7214.
- [11] CMS Collaboration, “Observation of a new boson at a mass of 125 GeV with the CMS experiment at the LHC”, *Phys. Lett. B* **716** (2012) 30, doi:10.1016/j.physletb.2012.08.021, arXiv:1207.7235.
- [12] CMS Collaboration, “Observation of a new boson with mass near 125 GeV in pp collisions at $\sqrt{s} = 7$ and 8 TeV”, *JHEP* **06** (2013) 081, doi:10.1007/JHEP06(2013)081, arXiv:1303.4571.
- [13] B. de Carlos and J. A. Casas, “One loop analysis of the electroweak breaking in supersymmetric models and the fine tuning problem”, *Phys. Lett. B* **309** (1993) 320, doi:10.1016/0370-2693(93)90940-J, arXiv:hep-ph/9303291.
- [14] G. W. Anderson and D. J. Castano, “Measures of fine tuning”, *Phys. Lett. B* **347** (1995) 300, doi:10.1016/0370-2693(95)00051-L, arXiv:hep-ph/9409419.
- [15] R. Kitano and Y. Nomura, “A Solution to the supersymmetric fine-tuning problem within the MSSM”, *Phys. Lett. B* **631** (2005) 58, doi:10.1016/j.physletb.2005.10.003, arXiv:hep-ph/0509039.

- [16] M. Asano, H. D. Kim, R. Kitano, and Y. Shimizu, “Natural supersymmetry at the LHC”, *JHEP* **12** (2010) 019, doi:[10.1007/JHEP12\(2010\)019](https://doi.org/10.1007/JHEP12(2010)019), arXiv:[1010.0692](https://arxiv.org/abs/1010.0692).
- [17] A. Strumia, “The Fine-tuning price of the early LHC”, *JHEP* **04** (2011) 073, doi:[10.1007/JHEP04\(2011\)073](https://doi.org/10.1007/JHEP04(2011)073), arXiv:[1101.2195](https://arxiv.org/abs/1101.2195).
- [18] M. Papucci, J. T. Ruderman, and A. Weiler, “Natural SUSY Endures”, *JHEP* **09** (2012) 035, doi:[10.1007/JHEP09\(2012\)035](https://doi.org/10.1007/JHEP09(2012)035), arXiv:[1110.6926](https://arxiv.org/abs/1110.6926).
- [19] CMS Collaboration, “Search for top-squark pair production in the single-lepton final state in pp collisions at $\sqrt{s} = 8$ TeV”, *Eur. Phys. J. C* **73** (2013) 2677, doi:[10.1140/epjc/s10052-013-2677-2](https://doi.org/10.1140/epjc/s10052-013-2677-2), arXiv:[1308.1586](https://arxiv.org/abs/1308.1586).
- [20] CMS Collaboration, “Search for gluino mediated bottom- and top-squark production in multijet final states in pp collisions at 8 TeV”, *Phys. Lett. B* **725** (2013) 243, doi:[10.1016/j.physletb.2013.06.058](https://doi.org/10.1016/j.physletb.2013.06.058), arXiv:[1305.2390](https://arxiv.org/abs/1305.2390).
- [21] CMS Collaboration, “Search for new physics in the multijet and missing transverse momentum final state in proton-proton collisions at $\sqrt{s} = 8$ TeV”, *JHEP* **06** (2014) 055, doi:[10.1007/JHEP06\(2014\)055](https://doi.org/10.1007/JHEP06(2014)055), arXiv:[1402.4770](https://arxiv.org/abs/1402.4770).
- [22] CMS Collaboration, “Search for supersymmetry in pp collisions at $\sqrt{s} = 8$ TeV in events with a single lepton, large jet multiplicity, and multiple b jets”, *Phys. Lett. B* **733** (2014) 328, doi:[10.1016/j.physletb.2014.04.023](https://doi.org/10.1016/j.physletb.2014.04.023), arXiv:[1311.4937](https://arxiv.org/abs/1311.4937).
- [23] CMS Collaboration, “Search for new physics in events with same-sign dileptons and jets in pp collisions at $\sqrt{s} = 8$ TeV”, *JHEP* **01** (2014) 163, doi:[10.1007/JHEP01\(2014\)163](https://doi.org/10.1007/JHEP01(2014)163), arXiv:[1311.6736](https://arxiv.org/abs/1311.6736).
- [24] ATLAS Collaboration, “Search for new phenomena in final states with large jet multiplicities and missing transverse momentum at $\sqrt{s} = 8$ TeV proton-proton collisions using the ATLAS experiment”, *JHEP* **10** (2013) 130, doi:[10.1007/JHEP10\(2013\)130](https://doi.org/10.1007/JHEP10(2013)130), arXiv:[1308.1841](https://arxiv.org/abs/1308.1841).
- [25] ATLAS Collaboration, “Search for strong production of supersymmetric particles in final states with missing transverse momentum and at least three b-jets at $\sqrt{s} = 8$ TeV proton-proton collisions with the ATLAS detector”, *JHEP* **10** (2014) 24, doi:[10.1007/JHEP10\(2014\)024](https://doi.org/10.1007/JHEP10(2014)024), arXiv:[1407.0600](https://arxiv.org/abs/1407.0600).
- [26] ATLAS Collaboration, “Search for supersymmetry at $\sqrt{s} = 8$ TeV in final states with jets and two same-sign leptons or three leptons with the ATLAS detector”, *JHEP* **06** (2014) 035, doi:[10.1007/JHEP06\(2014\)035](https://doi.org/10.1007/JHEP06(2014)035), arXiv:[1404.2500](https://arxiv.org/abs/1404.2500).
- [27] ATLAS Collaboration, “Search for direct pair production of the top squark in all-hadronic final states in proton-proton collisions at $\sqrt{s} = 8$ TeV with the ATLAS detector”, *JHEP* **09** (2014) 015, doi:[10.1007/JHEP09\(2014\)015](https://doi.org/10.1007/JHEP09(2014)015), arXiv:[1406.1122](https://arxiv.org/abs/1406.1122).
- [28] ATLAS Collaboration, “Search for direct top-squark pair production in final states with two leptons in pp collisions at $\sqrt{s} = 8$ TeV with the ATLAS detector”, *JHEP* **06** (2014) 124, doi:[10.1007/JHEP06\(2014\)124](https://doi.org/10.1007/JHEP06(2014)124), arXiv:[1403.4853](https://arxiv.org/abs/1403.4853).
- [29] N. Arkani-Hamed et al., “MAMBOSET: The Path from LHC Data to the New Standard Model via On-Shell Effective Theories”, (2007). arXiv:[hep-ph/0703088](https://arxiv.org/abs/hep-ph/0703088).

- [30] J. Alwall, P. C. Schuster, and N. Toro, “Simplified models for a first characterization of new physics at the LHC”, *Phys. Rev. D* **79** (2009) 075020,
[doi:10.1103/PhysRevD.79.075020](https://doi.org/10.1103/PhysRevD.79.075020), arXiv:0810.3921.
- [31] J. Alwall, M.-P. Le, M. Lisanti, and J. G. Wacker, “Model independent jets plus missing energy searches”, *Phys. Rev. D* **79** (2009) 015005,
[doi:10.1103/PhysRevD.79.015005](https://doi.org/10.1103/PhysRevD.79.015005), arXiv:0809.3264.
- [32] D. S. M. Alves, E. Izaguirre, and J. G. Wacker, “Where the sidewalk ends: jets and missing energy search strategies for the 7 TeV LHC”, *JHEP* **10** (2011) 012,
[doi:10.1007/JHEP10\(2011\)012](https://doi.org/10.1007/JHEP10(2011)012), arXiv:1102.5338.
- [33] LHC New Physics Working Group Collaboration, “Simplified models for LHC new physics searches”, *J. Phys. G* **39** (2012) 105005,
[doi:10.1088/0954-3899/39/10/105005](https://doi.org/10.1088/0954-3899/39/10/105005), arXiv:1105.2838.
- [34] M. L. Graesser and J. Shelton, “Hunting Mixed Top Squark Decays”, *Phys. Rev. Lett.* **111** (2013) 121802, doi:10.1103/PhysRevLett.111.121802, arXiv:1212.4495.
- [35] C. Rogan, “Kinematics for new dynamics at the LHC”, (2010). arXiv:1006.2727.
- [36] CMS Collaboration, “Inclusive search for squarks and gluinos in pp collisions at $\sqrt{s} = 7$ TeV”, *Phys. Rev. D* **85** (2012) 012004, doi:10.1103/PhysRevD.85.012004, arXiv:1107.1279.
- [37] CMS Collaboration, “Inclusive Search for Supersymmetry Using Razor Variables in pp Collisions at $\sqrt{s} = 7$ TeV”, *Phys. Rev. Lett.* **111** (2013) 081802,
[doi:10.1103/PhysRevLett.111.081802](https://doi.org/10.1103/PhysRevLett.111.081802), arXiv:1212.6961.
- [38] CMS Collaboration, “Search for supersymmetry with razor variables in pp collisions at $\sqrt{s} = 7$ TeV”, *Phys. Rev. D* **90** (2014), no. 11, 112001,
[doi:10.1103/PhysRevD.90.112001](https://doi.org/10.1103/PhysRevD.90.112001), arXiv:1405.3961.
- [39] ATLAS Collaboration, “Multi-channel search for squarks and gluinos in $\sqrt{s} = 7$ TeV pp collisions with the ATLAS detector”, *Eur. Phys. J. C* **73** (2013) 2362,
[doi:10.1140/epjc/s10052-013-2362-5](https://doi.org/10.1140/epjc/s10052-013-2362-5), arXiv:1212.6149.
- [40] ATLAS and CMS Collaborations, “Procedure for the LHC Higgs boson search combination in Summer 2011”, CMS Note/ATLAS Pub CMS-NOTE-2011-005, ATL-PHYS-PUB-2011-11, 2011.
- [41] CMS Collaboration, “Interpretation of Searches for Supersymmetry with Simplified Models”, *Phys. Rev. D* **88** (2013) 052017, doi:10.1103/PhysRevD.88.052017, arXiv:1301.2175.
- [42] J. Alwall et al., “MadGraph5: going beyond”, *JHEP* **06** (2011) 128,
[doi:10.1007/JHEP06\(2011\)128](https://doi.org/10.1007/JHEP06(2011)128), arXiv:1106.0522.
- [43] J. Alwall et al., “The automated computation of tree-level and next-to-leading order differential cross sections, and their matching to parton shower simulations”, *JHEP* **07** (2014) 079, doi:10.1007/JHEP07(2014)079, arXiv:1405.0301.
- [44] S. Höche et al., “Matching parton showers and matrix elements”, (2006). arXiv:hep-ph/0602031.

- [45] CMS Collaboration, “The fast simulation of the CMS detector at LHC”, *J. Phys.: Conf. Ser.* **331** (2011) 032049, doi:10.1088/1742-6596/331/3/032049.
- [46] W. Beenakker, R. Höpker, M. Spira, and P. M. Zerwas, “Squark and gluino production at hadron colliders”, *Nucl. Phys. B* **492** (1997) 51, doi:10.1016/S0550-3213(97)80027-2, arXiv:hep-ph/9610490.
- [47] A. Kulesza and L. Motyka, “Threshold Resummation for Squark-Antisquark and Gluino-Pair Production at the LHC”, *Phys. Rev. Lett.* **102** (2009) 111802, doi:10.1103/PhysRevLett.102.111802, arXiv:0807.2405.
- [48] A. Kulesza and L. Motyka, “Soft gluon resummation for the production of gluino-gluino and squark-antisquark pairs at the LHC”, *Phys. Rev. D* **80** (2009) 095004, doi:10.1103/PhysRevD.80.095004, arXiv:0905.4749.
- [49] W. Beenakker et al., “Soft-gluon resummation for squark and gluino hadroproduction”, *JHEP* **12** (2009) 041, doi:10.1088/1126-6708/2009/12/041, arXiv:0909.4418.
- [50] W. Beenakker et al., “Squark and gluino hadroproduction”, *Int. J. Mod. Phys. A* **26** (2011) 2637, doi:10.1142/S0217751X11053560, arXiv:1105.1110.
- [51] M. Krämer et al., “Supersymmetry production cross sections in pp collisions at $\sqrt{s} = 7$ TeV”, (2012). arXiv:1206.2892.
- [52] CMS Collaboration, “The CMS experiment at the CERN LHC”, *JINST* **3** (2008) S08004, doi:10.1088/1748-0221/3/08/S08004.
- [53] CMS Collaboration, “Missing transverse energy performance of the CMS detector”, *JINST* **6** (2011) P09001, doi:10.1088/1748-0221/6/09/P09001, arXiv:1106.5048.
- [54] CMS Collaboration, “Search for New Physics in the Multijet and Missing Transverse Momentum Final State in Proton-Proton Collisions at $\sqrt{s} = 7$ TeV”, *Phys. Rev. Lett.* **109** (2012) 171803, doi:10.1103/PhysRevLett.109.171803, arXiv:1207.1898.
- [55] CMS Collaboration, “Performance of the missing transverse energy reconstruction by the CMS experiment in $\sqrt{s} = 8$ TeV pp data”, CMS Physics Analysis Summary CMS-PAS-JME-13-003, 2013.
- [56] CMS Collaboration, “Particle-flow event reconstruction in CMS and performance for jets, taus, and E_T^{miss} ”, CMS Physics Analysis Summary CMS-PAS-PFT-09-001, 2009.
- [57] CMS Collaboration, “Commissioning of the particle-flow event reconstruction with the first LHC collisions recorded in the CMS detector”, CMS Physics Analysis Summary CMS-PAS-PFT-10-011, 2010.
- [58] M. Cacciari, G. P. Salam, and G. Soyez, “The catchment area of jets”, *JHEP* **04** (2008) 005, doi:10.1088/1126-6708/2008/04/005, arXiv:0802.1188.
- [59] M. Cacciari and G. P. Salam, “Pileup subtraction using jet areas”, *Phys. Lett. B* **659** (2008) 119, doi:10.1016/j.physletb.2007.09.077, arXiv:0707.1378.
- [60] CMS Collaboration, “Determination of jet energy calibration and transverse momentum resolution in CMS”, *JINST* **6** (2011) P11002, doi:10.1088/1748-0221/6/11/P11002.

- [61] CMS Collaboration, “Measurement of Higgs boson production and properties in the WW decay channel with leptonic final states”, *JHEP* **01** (2014) 096, doi:10.1007/JHEP01(2014)096, arXiv:1312.1129.
- [62] CMS Collaboration, “Measurement of the properties of a Higgs boson in the four-lepton final state”, *Phys. Rev. D* **89** (2014) 092007, doi:10.1103/PhysRevD.89.092007, arXiv:1312.5353.
- [63] M. Cacciari, G. P. Salam, and G. Soyez, “FastJet user manual”, *Eur. Phys. J. C* **72** (2012) 1896, doi:10.1140/epjc/s10052-012-1896-2, arXiv:1111.6097.
- [64] M. Cacciari, G. P. Salam, and G. Soyez, “The anti- k_T jet clustering algorithm”, *JHEP* **04** (2008) 063, doi:10.1088/1126-6708/2008/04/063, arXiv:0802.1189.
- [65] CMS Collaboration, “Performance of b tagging at $\sqrt{s} = 8$ TeV in multijet, $t\bar{t}$ and boosted topology events”, CMS Physics Analysis Summary CMS-PAS-BTV-13-001, 2013.
- [66] T. Sjöstrand, S. Mrenna, and P. Skands, “PYTHIA 6.4 physics and manual”, *JHEP* **05** (2006) 026, doi:10.1088/1126-6708/2006/05/026, arXiv:hep-ph/0603175.
- [67] GEANT4 Collaboration, “GEANT4—a simulation toolkit”, *Nucl. Instrum. Meth. A* **506** (2003) 250, doi:10.1016/S0168-9002(03)01368-8.
- [68] W. Verkerke and D. P. Kirkby, “The RooFit toolkit for data modeling”, in *2003 Computing in High Energy and Nuclear Physics (CHEP03)*, p. 186. 2003. arXiv:physics/0306116. eConf C0303241 (2003) MOLT007.
- [69] CMS Collaboration, “CMS Luminosity Based on Pixel Cluster Counting - Summer 2013 Update”, CMS Physics Analysis Summary CMS-PAS-LUM-13-001, 2013.
- [70] D. Bourilkov, R. C. Group, and M. R. Whalley, “LHAPDF: PDF use from the Tevatron to the LHC”, (2006). arXiv:hep-ph/0605240.
- [71] S. Alekhin et al., “The PDF4LHC Working Group Interim Report”, (2011). arXiv:1101.0536.
- [72] M. Botje et al., “The PDF4LHC Working Group Interim Recommendations”, (2011). arXiv:1101.0538.
- [73] P. M. Nadolsky et al., “Implications of CTEQ global analysis for collider observables”, *Phys. Rev. D* **78** (2008) 013004, doi:10.1103/PhysRevD.78.013004, arXiv:0802.0007.
- [74] A. D. Martin, W. J. Stirling, R. S. Thorne, and G. Watt, “Update of parton distributions at NNLO”, *Phys. Lett. B* **652** (2007) 292, doi:10.1016/j.physletb.2007.07.040, arXiv:0706.0459.

A The CMS Collaboration

Yerevan Physics Institute, Yerevan, Armenia
V. Khachatryan, A.M. Sirunyan, A. Tumasyan

Institut für Hochenergiephysik der OeAW, Wien, Austria

W. Adam, T. Bergauer, M. Dragicevic, J. Erö, M. Friedl, R. Frühwirth¹, V.M. Ghete, C. Hartl, N. Hörmann, J. Hrubec, M. Jeitler¹, W. Kiesenhofer, V. Knünz, M. Krammer¹, I. Krätschmer, D. Liko, I. Mikulec, D. Rabady², B. Rahbaran, H. Rohringer, R. Schöfbeck, J. Strauss, W. Treberer-Treberspurg, W. Waltenberger, C.-E. Wulz¹

National Centre for Particle and High Energy Physics, Minsk, Belarus

V. Mossolov, N. Shumeiko, J. Suarez Gonzalez

Universiteit Antwerpen, Antwerpen, Belgium

S. Alderweireldt, S. Bansal, T. Cornelis, E.A. De Wolf, X. Janssen, A. Knutsson, J. Lauwers, S. Luyckx, S. Ochesanu, R. Rougny, M. Van De Klundert, H. Van Haevermaet, P. Van Mechelen, N. Van Remortel, A. Van Spilbeeck

Vrije Universiteit Brussel, Brussel, Belgium

F. Blekman, S. Blyweert, J. D'Hondt, N. Daci, N. Heracleous, J. Keaveney, S. Lowette, M. Maes, A. Olbrechts, Q. Python, D. Strom, S. Tavernier, W. Van Doninck, P. Van Mulders, G.P. Van Onsem, I. Villella

Université Libre de Bruxelles, Bruxelles, Belgium

C. Caillol, B. Clerbaux, G. De Lentdecker, D. Dobur, L. Favart, A.P.R. Gay, A. Grebenyuk, A. Léonard, A. Mohammadi, L. Perniè², A. Randle-conde, T. Reis, T. Seva, L. Thomas, C. Vander Velde, P. Vanlaer, J. Wang, F. Zenoni

Ghent University, Ghent, Belgium

V. Adler, K. Beernaert, L. Benucci, A. Cimmino, S. Costantini, S. Crucy, S. Dildick, A. Fagot, G. Garcia, J. Mccartin, A.A. Ocampo Rios, D. Poyraz, D. Ryckbosch, S. Salva Diblen, M. Sigamani, N. Strobbe, F. Thyssen, M. Tytgat, E. Yazgan, N. Zaganidis

Université Catholique de Louvain, Louvain-la-Neuve, Belgium

S. Basegmez, C. Beluffi³, G. Bruno, R. Castello, A. Caudron, L. Ceard, G.G. Da Silveira, C. Delaere, T. du Pree, D. Favart, L. Forthomme, A. Giannanco⁴, J. Hollar, A. Jafari, P. Jez, M. Komm, V. Lemaitre, C. Nuttens, L. Perrini, A. Pin, K. Piotrkowski, A. Popov⁵, L. Quertenmont, M. Selvaggi, M. Vidal Marono, J.M. Vizan Garcia

Université de Mons, Mons, Belgium

N. Belyi, T. Caebergs, E. Daubie, G.H. Hammad

Centro Brasileiro de Pesquisas Fisicas, Rio de Janeiro, Brazil

W.L. Aldá Júnior, G.A. Alves, L. Brito, M. Correa Martins Junior, T. Dos Reis Martins, J. Molina, C. Mora Herrera, M.E. Pol, P. Rebello Teles

Universidade do Estado do Rio de Janeiro, Rio de Janeiro, Brazil

W. Carvalho, J. Chinellato⁶, A. Custódio, E.M. Da Costa, D. De Jesus Damiao, C. De Oliveira Martins, S. Fonseca De Souza, H. Malbouisson, D. Matos Figueiredo, L. Mundim, H. Nogima, W.L. Prado Da Silva, J. Santaolalla, A. Santoro, A. Sznajder, E.J. Tonelli Manganote⁶, A. Vilela Pereira

Universidade Estadual Paulista ^a, Universidade Federal do ABC ^b, São Paulo, Brazil
 C.A. Bernardes^b, S. Dogra^a, T.R. Fernandez Perez Tomei^a, E.M. Gregores^b, P.G. Mercadante^b,
 S.F. Novaes^a, Sandra S. Padula^a

Institute for Nuclear Research and Nuclear Energy, Sofia, Bulgaria
 A. Aleksandrov, V. Genchev², R. Hadjiiska, P. Iaydjiev, A. Marinov, S. Piperov, M. Rodozov,
 S. Stoykova, G. Sultanov, M. Vutova

University of Sofia, Sofia, Bulgaria
 A. Dimitrov, I. Glushkov, L. Litov, B. Pavlov, P. Petkov

Institute of High Energy Physics, Beijing, China
 J.G. Bian, G.M. Chen, H.S. Chen, M. Chen, T. Cheng, R. Du, C.H. Jiang, R. Plestina⁷, F. Romeo,
 J. Tao, Z. Wang

State Key Laboratory of Nuclear Physics and Technology, Peking University, Beijing, China
 C. Asawatangtrakuldee, Y. Ban, Q. Li, S. Liu, Y. Mao, S.J. Qian, D. Wang, Z. Xu, W. Zou

Universidad de Los Andes, Bogota, Colombia
 C. Avila, A. Cabrera, L.F. Chaparro Sierra, C. Florez, J.P. Gomez, B. Gomez Moreno,
 J.C. Sanabria

**University of Split, Faculty of Electrical Engineering, Mechanical Engineering and Naval
 Architecture, Split, Croatia**
 N. Godinovic, D. Lelas, D. Polic, I. Puljak

University of Split, Faculty of Science, Split, Croatia
 Z. Antunovic, M. Kovac

Institute Rudjer Boskovic, Zagreb, Croatia
 V. Brigljevic, K. Kadija, J. Luetic, D. Mekterovic, L. Sudic

University of Cyprus, Nicosia, Cyprus
 A. Attikis, G. Mavromanolakis, J. Mousa, C. Nicolaou, F. Ptochos, P.A. Razis

Charles University, Prague, Czech Republic
 M. Bodlak, M. Finger, M. Finger Jr.⁸

**Academy of Scientific Research and Technology of the Arab Republic of Egypt, Egyptian
 Network of High Energy Physics, Cairo, Egypt**
 Y. Assran⁹, A. Ellithi Kamel¹⁰, M.A. Mahmoud¹¹, A. Radi^{12,13}

National Institute of Chemical Physics and Biophysics, Tallinn, Estonia
 M. Kadastik, M. Murumaa, M. Raidal, A. Tiko

Department of Physics, University of Helsinki, Helsinki, Finland
 P. Eerola, M. Voutilainen

Helsinki Institute of Physics, Helsinki, Finland
 J. Hätkönen, V. Karimäki, R. Kinnunen, M.J. Kortelainen, T. Lampén, K. Lassila-Perini, S. Lehti,
 T. Lindén, P. Luukka, T. Mäenpää, T. Peltola, E. Tuominen, J. Tuominiemi, E. Tuovinen,
 L. Wendland

Lappeenranta University of Technology, Lappeenranta, Finland
 J. Talvitie, T. Tuuva

DSM/IRFU, CEA/Saclay, Gif-sur-Yvette, France

M. Besancon, F. Couderc, M. Dejardin, D. Denegri, B. Fabbro, J.L. Faure, C. Favaro, F. Ferri, S. Ganjour, A. Givernaud, P. Gras, G. Hamel de Monchenault, P. Jarry, E. Locci, J. Malcles, J. Rander, A. Rosowsky, M. Titov

Laboratoire Leprince-Ringuet, Ecole Polytechnique, IN2P3-CNRS, Palaiseau, France

S. Baffioni, F. Beaudette, P. Busson, E. Chapon, C. Charlot, T. Dahms, M. Dalchenko, L. Dobrzynski, N. Filipovic, A. Florent, R. Granier de Cassagnac, L. Mastrolorenzo, P. Miné, I.N. Naranjo, M. Nguyen, C. Ochando, G. Ortona, P. Paganini, S. Regnard, R. Salerno, J.B. Sauvan, Y. Sirois, C. Veelken, Y. Yilmaz, A. Zabi

Institut Pluridisciplinaire Hubert Curien, Université de Strasbourg, Université de Haute Alsace Mulhouse, CNRS/IN2P3, Strasbourg, France

J.-L. Agram¹⁴, J. Andrea, A. Aubin, D. Bloch, J.-M. Brom, E.C. Chabert, C. Collard, E. Conte¹⁴, J.-C. Fontaine¹⁴, D. Gelé, U. Goerlach, C. Goetzmann, A.-C. Le Bihan, K. Skovpen, P. Van Hove

Centre de Calcul de l’Institut National de Physique Nucléaire et de Physique des Particules, CNRS/IN2P3, Villeurbanne, France

S. Gadrat

Université de Lyon, Université Claude Bernard Lyon 1, CNRS-IN2P3, Institut de Physique Nucléaire de Lyon, Villeurbanne, France

S. Beauceron, N. Beaupere, C. Bernet⁷, G. Boudoul², E. Bouvier, S. Brochet, C.A. Carrillo Montoya, J. Chasserat, R. Chierici, D. Contardo², P. Depasse, H. El Mamouni, J. Fan, J. Fay, S. Gascon, M. Gouzevitch, B. Ille, T. Kurca, M. Lethuillier, L. Mirabito, S. Perries, J.D. Ruiz Alvarez, D. Sabes, L. Sgandurra, V. Sordini, M. Vander Donckt, P. Verdier, S. Viret, H. Xiao

Institute of High Energy Physics and Informatization, Tbilisi State University, Tbilisi, Georgia

Z. Tsamalaidze⁸

RWTH Aachen University, I. Physikalisches Institut, Aachen, Germany

C. Autermann, S. Beranek, M. Bortenackels, M. Edelhoff, L. Feld, A. Heister, K. Klein, M. Lipinski, A. Ostapchuk, M. Preuten, F. Raupach, J. Sammet, S. Schael, J.F. Schulte, H. Weber, B. Wittmer, V. Zhukov⁵

RWTH Aachen University, III. Physikalisches Institut A, Aachen, Germany

M. Ata, M. Brodski, E. Dietz-Laursonn, D. Duchardt, M. Erdmann, R. Fischer, A. Güth, T. Hebbeker, C. Heidemann, K. Hoepfner, D. Klingebiel, S. Knutzen, P. Kreuzer, M. Merschmeyer, A. Meyer, P. Millet, M. Olschewski, K. Padeken, P. Papacz, H. Reithler, S.A. Schmitz, L. Sonnenschein, D. Teyssier, S. Thüer, M. Weber

RWTH Aachen University, III. Physikalisches Institut B, Aachen, Germany

V. Cherepanov, Y. Erdogan, G. Flügge, H. Geenen, M. Geisler, W. Haj Ahmad, F. Hoehle, B. Kargoll, T. Kress, Y. Kuessel, A. Künsken, J. Lingemann², A. Nowack, I.M. Nugent, O. Pooth, A. Stahl

Deutsches Elektronen-Synchrotron, Hamburg, Germany

M. Aldaya Martin, I. Asin, N. Bartosik, J. Behr, U. Behrens, A.J. Bell, A. Bethani, K. Borras, A. Burgmeier, A. Cakir, L. Calligaris, A. Campbell, S. Choudhury, F. Costanza, C. Diez Pardos, G. Dolinska, S. Dooling, T. Dorland, G. Eckerlin, D. Eckstein, T. Eichhorn, G. Flucke, J. Garay Garcia, A. Geiser, A. Gzhko, P. Gunnellini, J. Hauk, M. Hempel¹⁵, H. Jung, A. Kalogeropoulos, M. Kasemann, P. Katsas, J. Kieseler, C. Kleinwort, I. Korol, D. Krücker, W. Lange, J. Leonard, K. Lipka, A. Lobanov, W. Lohmann¹⁵, B. Lutz, R. Mankel, I. Marfin¹⁵, I.-A. Melzer-Pellmann,

A.B. Meyer, G. Mittag, J. Mnich, A. Mussgiller, S. Naumann-Emme, A. Nayak, E. Ntomari, H. Perrey, D. Pitzl, R. Placakyte, A. Raspereza, P.M. Ribeiro Cipriano, B. Roland, E. Ron, M.Ö. Sahin, J. Salfeld-Nebgen, P. Saxena, T. Schoerner-Sadenius, M. Schröder, C. Seitz, S. Spannagel, A.D.R. Vargas Trevino, R. Walsh, C. Wissing

University of Hamburg, Hamburg, Germany

V. Blobel, M. Centis Vignali, A.R. Draeger, J. Erfle, E. Garutti, K. Goebel, M. Görner, J. Haller, M. Hoffmann, R.S. Höing, A. Junkes, H. Kirschenmann, R. Klanner, R. Kogler, J. Lange, T. Lapsien, T. Lenz, I. Marchesini, J. Ott, T. Peiffer, A. Perieanu, N. Pietsch, J. Poehlsen, T. Poehlsen, D. Rathjens, C. Sander, H. Schettler, P. Schleper, E. Schlieckau, A. Schmidt, M. Seidel, V. Sola, H. Stadie, G. Steinbrück, D. Troendle, E. Usai, L. Vanelder, A. Vanhoefer

Institut für Experimentelle Kernphysik, Karlsruhe, Germany

C. Barth, C. Baus, J. Berger, C. Böser, E. Butz, T. Chwalek, W. De Boer, A. Descroix, A. Dierlamm, M. Feindt, F. Freisch, M. Giffels, A. Gilbert, F. Hartmann², T. Hauth, U. Husemann, I. Katkov⁵, A. Kornmayer², P. Lobelle Pardo, M.U. Mozer, T. Müller, Th. Müller, A. Nürnberg, G. Quast, K. Rabbertz, S. Röcker, H.J. Simonis, F.M. Stober, R. Ulrich, J. Wagner-Kuhr, S. Wayand, T. Weiler, R. Wolf

Institute of Nuclear and Particle Physics (INPP), NCSR Demokritos, Aghia Paraskevi, Greece

G. Anagnostou, G. Daskalakis, T. Geralis, V.A. Giakoumopoulou, A. Kyriakis, D. Loukas, A. Markou, C. Markou, A. Psallidas, I. Topsis-Giotis

University of Athens, Athens, Greece

A. Agapitos, S. Kesisoglou, A. Panagiotou, N. Saoulidou, E. Stiliaris

University of Ioánnina, Ioánnina, Greece

X. Aslanoglou, I. Evangelou, G. Flouris, C. Foudas, P. Kokkas, N. Manthos, I. Papadopoulos, E. Paradas, J. Strologas

Wigner Research Centre for Physics, Budapest, Hungary

G. Bencze, C. Hajdu, P. Hidas, D. Horvath¹⁶, F. Sikler, V. Veszpreni, G. Vesztergombi¹⁷, A.J. Zsigmond

Institute of Nuclear Research ATOMKI, Debrecen, Hungary

N. Beni, S. Czellar, J. Karancsi¹⁸, J. Molnar, J. Palinkas, Z. Szillasi

University of Debrecen, Debrecen, Hungary

A. Makovec, P. Raics, Z.L. Trocsanyi, B. Ujvari

National Institute of Science Education and Research, Bhubaneswar, India

S.K. Swain

Panjab University, Chandigarh, India

S.B. Beri, V. Bhatnagar, R. Gupta, U.Bhawandeep, A.K. Kalsi, M. Kaur, R. Kumar, M. Mittal, N. Nishu, J.B. Singh

University of Delhi, Delhi, India

Ashok Kumar, Arun Kumar, S. Ahuja, A. Bhardwaj, B.C. Choudhary, A. Kumar, S. Malhotra, M. Naimuddin, K. Ranjan, V. Sharma

Saha Institute of Nuclear Physics, Kolkata, India

S. Banerjee, S. Bhattacharya, K. Chatterjee, S. Dutta, B. Gomber, Sa. Jain, Sh. Jain, R. Khurana, A. Modak, S. Mukherjee, D. Roy, S. Sarkar, M. Sharan

Bhabha Atomic Research Centre, Mumbai, India

A. Abdulsalam, D. Dutta, V. Kumar, A.K. Mohanty², L.M. Pant, P. Shukla, A. Topkar

Tata Institute of Fundamental Research, Mumbai, India

T. Aziz, S. Banerjee, S. Bhowmik¹⁹, R.M. Chatterjee, R.K. Dewanjee, S. Dugad, S. Ganguly, S. Ghosh, M. Guchait, A. Gurtu²⁰, G. Kole, S. Kumar, M. Maity¹⁹, G. Majumder, K. Mazumdar, G.B. Mohanty, B. Parida, K. Sudhakar, N. Wickramage²¹

Institute for Research in Fundamental Sciences (IPM), Tehran, Iran

H. Bakhshiansohi, H. Behnamian, S.M. Etesami²², A. Fahim²³, R. Goldouzian, M. Khakzad, M. Mohammadi Najafabadi, M. Naseri, S. Pakhtinat Mehdiabadi, F. Rezaei Hosseinabadi, B. Safarzadeh²⁴, M. Zeinali

University College Dublin, Dublin, Ireland

M. Felcini, M. Grunewald

INFN Sezione di Bari ^a, Università di Bari ^b, Politecnico di Bari ^c, Bari, Italy

M. Abbrescia^{a,b}, C. Calabria^{a,b}, S.S. Chhibra^{a,b}, A. Colaleo^a, D. Creanza^{a,c}, N. De Filippis^{a,c}, M. De Palma^{a,b}, L. Fiore^a, G. Iaselli^{a,c}, G. Maggi^{a,c}, M. Maggi^a, S. My^{a,c}, S. Nuzzo^{a,b}, A. Pompili^{a,b}, G. Pugliese^{a,c}, R. Radogna^{a,b,2}, G. Selvaggi^{a,b}, A. Sharma^a, L. Silvestris^{a,2}, R. Venditti^{a,b}, P. Verwilligen^a

INFN Sezione di Bologna ^a, Università di Bologna ^b, Bologna, Italy

G. Abbiendi^a, A.C. Benvenuti^a, D. Bonacorsi^{a,b}, S. Braibant-Giacomelli^{a,b}, L. Brigliadori^{a,b}, R. Campanini^{a,b}, P. Capiluppi^{a,b}, A. Castro^{a,b}, F.R. Cavallo^a, G. Codispoti^{a,b}, M. Cuffiani^{a,b}, G.M. Dallavalle^a, F. Fabbri^a, A. Fanfani^{a,b}, D. Fasanella^{a,b}, P. Giacomelli^a, C. Grandi^a, L. Guiducci^{a,b}, S. Marcellini^a, G. Masetti^a, A. Montanari^a, F.L. Navarria^{a,b}, A. Perrotta^a, A.M. Rossi^{a,b}, T. Rovelli^{a,b}, G.P. Siroli^{a,b}, N. Tosi^{a,b}, R. Travaglini^{a,b}

INFN Sezione di Catania ^a, Università di Catania ^b, CSFNSM ^c, Catania, Italy

S. Albergo^{a,b}, G. Cappello^a, M. Chiorboli^{a,b}, S. Costa^{a,b}, F. Giordano^{a,c,2}, R. Potenza^{a,b}, A. Tricomi^{a,b}, C. Tuve^{a,b}

INFN Sezione di Firenze ^a, Università di Firenze ^b, Firenze, Italy

G. Barbagli^a, V. Ciulli^{a,b}, C. Civinini^a, R. D'Alessandro^{a,b}, E. Focardi^{a,b}, E. Gallo^a, S. Gonzi^{a,b}, V. Gori^{a,b}, P. Lenzi^{a,b}, M. Meschini^a, S. Paoletti^a, G. Sguazzoni^a, A. Tropiano^{a,b}

INFN Laboratori Nazionali di Frascati, Frascati, Italy

L. Benussi, S. Bianco, F. Fabbri, D. Piccolo

INFN Sezione di Genova ^a, Università di Genova ^b, Genova, Italy

R. Ferretti^{a,b}, F. Ferro^a, M. Lo Vetere^{a,b}, E. Robutti^a, S. Tosi^{a,b}

INFN Sezione di Milano-Bicocca ^a, Università di Milano-Bicocca ^b, Milano, Italy

M.E. Dinardo^{a,b}, S. Fiorendi^{a,b}, S. Gennai^{a,2}, R. Gerosa^{a,b,2}, A. Ghezzi^{a,b}, P. Govoni^{a,b}, M.T. Lucchini^{a,b,2}, S. Malvezzi^a, R.A. Manzoni^{a,b}, A. Martelli^{a,b}, B. Marzocchi^{a,b,2}, D. Menasce^a, L. Moroni^a, M. Paganoni^{a,b}, D. Pedrini^a, S. Ragazzi^{a,b}, N. Redaelli^a, T. Tabarelli de Fatis^{a,b}

INFN Sezione di Napoli ^a, Università di Napoli 'Federico II' ^b, Università della Basilicata (Potenza) ^c, Università G. Marconi (Roma) ^d, Napoli, Italy

S. Buontempo^a, N. Cavallo^{a,c}, S. Di Guida^{a,d,2}, F. Fabozzi^{a,c}, A.O.M. Iorio^{a,b}, L. Lista^a, S. Meola^{a,d,2}, M. Merola^a, P. Paolucci^{a,2}

INFN Sezione di Padova ^a, Università di Padova ^b, Università di Trento (Trento) ^c, Padova, Italy

P. Azzi^a, N. Bacchetta^a, D. Bisello^{a,b}, A. Branca^{a,b}, R. Carlin^{a,b}, P. Checchia^a, M. Dall'Osso^{a,b}, T. Dorigo^a, U. Dosselli^a, M. Galanti^{a,b}, U. Gasparini^{a,b}, F. Gonella^a, A. Gozzelino^a, M. Gulmini^{a,25}, K. Kanishchev^{a,c}, S. Lacaprara^a, M. Margoni^{a,b}, A.T. Meneguzzo^{a,b}, J. Pazzini^{a,b}, N. Pozzobon^{a,b}, P. Ronchese^{a,b}, F. Simonetto^{a,b}, E. Torassa^a, M. Tosi^{a,b}, P. Zotto^{a,b}, A. Zucchetta^{a,b}

INFN Sezione di Pavia ^a, Università di Pavia ^b, Pavia, Italy

M. Gabusi^{a,b}, S.P. Ratti^{a,b}, V. Re^a, C. Riccardi^{a,b}, P. Salvini^a, P. Vitulo^{a,b}

INFN Sezione di Perugia ^a, Università di Perugia ^b, Perugia, Italy

M. Biasini^{a,b}, G.M. Bilei^a, D. Ciangottini^{a,b,2}, L. Fanò^{a,b}, P. Lariccia^{a,b}, G. Mantovani^{a,b}, M. Menichelli^a, A. Saha^a, A. Santocchia^{a,b}, A. Spiezzi^{a,b,2}

INFN Sezione di Pisa ^a, Università di Pisa ^b, Scuola Normale Superiore di Pisa ^c, Pisa, Italy

K. Androsov^{a,26}, P. Azzurri^a, G. Bagliesi^a, J. Bernardini^a, T. Boccali^a, G. Broccolo^{a,c}, R. Castaldi^a, M.A. Ciocci^{a,26}, R. Dell'Orso^a, S. Donato^{a,c,2}, G. Fedi, F. Fiori^{a,c}, L. Foà^{a,c}, A. Giassi^a, M.T. Grippo^{a,26}, F. Ligabue^{a,c}, T. Lomtadze^a, L. Martini^{a,b}, A. Messineo^{a,b}, C.S. Moon^{a,27}, F. Palla^{a,2}, A. Rizzi^{a,b}, A. Savoy-Navarro^{a,28}, A.T. Serban^a, P. Spagnolo^a, P. Squillaciotti^{a,26}, R. Tenchini^a, G. Tonelli^{a,b}, A. Venturi^a, P.G. Verdini^a, C. Vernieri^{a,c}

INFN Sezione di Roma ^a, Università di Roma ^b, Roma, Italy

L. Barone^{a,b}, F. Cavallari^a, G. D'imperio^{a,b}, D. Del Re^{a,b}, M. Diemoz^a, C. Jorda^a, E. Longo^{a,b}, F. Margaroli^{a,b}, P. Meridiani^a, F. Micheli^{a,b,2}, G. Organtini^{a,b}, R. Paramatti^a, S. Rahatlou^{a,b}, C. Rovelli^a, F. Santanastasio^{a,b}, L. Soffi^{a,b}, P. Traczyk^{a,b,2}

INFN Sezione di Torino ^a, Università di Torino ^b, Università del Piemonte Orientale (Novara) ^c, Torino, Italy

N. Amapane^{a,b}, R. Arcidiacono^{a,c}, S. Argiro^{a,b}, M. Arneodo^{a,c}, R. Bellan^{a,b}, C. Biino^a, N. Cartiglia^a, S. Casasso^{a,b,2}, M. Costa^{a,b}, A. Degano^{a,b}, N. Demaria^a, L. Finco^{a,b,2}, C. Mariotti^a, S. Maselli^a, E. Migliore^{a,b}, V. Monaco^{a,b}, M. Musich^a, M.M. Obertino^{a,c}, L. Pacher^{a,b}, N. Pastrone^a, M. Pelliccioni^a, G.L. Pinna Angioni^{a,b}, A. Potenza^{a,b}, A. Romero^{a,b}, M. Ruspa^{a,c}, R. Sacchi^{a,b}, A. Solano^{a,b}, A. Staiano^a, U. Tamponi^a

INFN Sezione di Trieste ^a, Università di Trieste ^b, Trieste, Italy

S. Belforte^a, V. Candelise^{a,b,2}, M. Casarsa^a, F. Cossutti^a, G. Della Ricca^{a,b}, B. Gobbo^a, C. La Licata^{a,b}, M. Marone^{a,b}, A. Schizzi^{a,b}, T. Umer^{a,b}, A. Zanetti^a

Kangwon National University, Chunchon, Korea

S. Chang, A. Kropivnitskaya, S.K. Nam

Kyungpook National University, Daegu, Korea

D.H. Kim, G.N. Kim, M.S. Kim, D.J. Kong, S. Lee, Y.D. Oh, H. Park, A. Sakharov, D.C. Son

Chonbuk National University, Jeonju, Korea

T.J. Kim, M.S. Ryu

Chonnam National University, Institute for Universe and Elementary Particles, Kwangju, Korea

J.Y. Kim, D.H. Moon, S. Song

Korea University, Seoul, Korea

S. Choi, D. Gyun, B. Hong, M. Jo, H. Kim, Y. Kim, B. Lee, K.S. Lee, S.K. Park, Y. Roh

Seoul National University, Seoul, Korea

H.D. Yoo

University of Seoul, Seoul, Korea

M. Choi, J.H. Kim, I.C. Park, G. Ryu

Sungkyunkwan University, Suwon, Korea

Y. Choi, Y.K. Choi, J. Goh, D. Kim, E. Kwon, J. Lee, I. Yu

Vilnius University, Vilnius, Lithuania

A. Juodagalvis

National Centre for Particle Physics, Universiti Malaya, Kuala Lumpur, Malaysia

J.R. Komaragiri, M.A.B. Md Ali

Centro de Investigacion y de Estudios Avanzados del IPN, Mexico City, Mexico

E. Casimiro Linares, H. Castilla-Valdez, E. De La Cruz-Burelo, I. Heredia-de La Cruz, A. Hernandez-Almada, R. Lopez-Fernandez, A. Sanchez-Hernandez

Universidad Iberoamericana, Mexico City, Mexico

S. Carrillo Moreno, F. Vazquez Valencia

Benemerita Universidad Autonoma de Puebla, Puebla, Mexico

I. Pedraza, H.A. Salazar Ibarguen

Universidad Autónoma de San Luis Potosí, San Luis Potosí, Mexico

A. Morelos Pineda

University of Auckland, Auckland, New Zealand

D. Kofcheck

University of Canterbury, Christchurch, New Zealand

P.H. Butler, S. Reucroft

National Centre for Physics, Quaid-I-Azam University, Islamabad, Pakistan

A. Ahmad, M. Ahmad, Q. Hassan, H.R. Hoorani, W.A. Khan, T. Khurshid, M. Shoaib

National Centre for Nuclear Research, Swierk, Poland

H. Bialkowska, M. Bluj, B. Boimska, T. Frueboes, M. Górska, M. Kazana, K. Nawrocki, K. Romanowska-Rybinska, M. Szleper, P. Zalewski

Institute of Experimental Physics, Faculty of Physics, University of Warsaw, Warsaw, Poland

G. Brona, K. Bunkowski, M. Cwiok, W. Dominik, K. Doroba, A. Kalinowski, M. Konecki, J. Krolikowski, M. Misiura, M. Olszewski

Laboratório de Instrumentação e Física Experimental de Partículas, Lisboa, Portugal

P. Bargassa, C. Beirão Da Cruz E Silva, P. Faccioli, P.G. Ferreira Parracho, M. Gallinaro, L. Lloret Iglesias, F. Nguyen, J. Rodrigues Antunes, J. Seixas, J. Varela, P. Vischia

Joint Institute for Nuclear Research, Dubna, RussiaS. Afanasiev, P. Bunin, M. Gavrilenko, I. Golutvin, I. Gorbunov, A. Kamenev, V. Karjavin, V. Konoplyanikov, A. Lanev, A. Malakhov, V. Matveev²⁹, P. Moisenz, V. Palichik, V. Perelygin, S. Shmatov, N. Skatchkov, V. Smirnov, A. Zarubin**Petersburg Nuclear Physics Institute, Gatchina (St. Petersburg), Russia**V. Golovtsov, Y. Ivanov, V. Kim³⁰, E. Kuznetsova, P. Levchenko, V. Murzin, V. Oreshkin, I. Smirnov, V. Sulimov, L. Uvarov, S. Vavilov, A. Vorobyev, An. Vorobyev

Institute for Nuclear Research, Moscow, Russia

Yu. Andreev, A. Dermenev, S. Glinenko, N. Golubev, M. Kirsanov, N. Krasnikov, A. Pashenkov, D. Tlisov, A. Toropin

Institute for Theoretical and Experimental Physics, Moscow, Russia

V. Epshteyn, V. Gavrilov, N. Lychkovskaya, V. Popov, I. Pozdnyakov, G. Safronov, S. Semenov, A. Spiridonov, V. Stolin, E. Vlasov, A. Zhokin

P.N. Lebedev Physical Institute, Moscow, Russia

V. Andreev, M. Azarkin³¹, I. Dremin³¹, M. Kirakosyan, A. Leonidov³¹, G. Mesyats, S.V. Rusakov, A. Vinogradov

Skobeltsyn Institute of Nuclear Physics, Lomonosov Moscow State University, Moscow, Russia

A. Belyaev, E. Boos, M. Dubinin³², L. Dudko, A. Ershov, A. Gribushin, V. Klyukhin, O. Kodolova, I. Lokhtin, S. Obraztsov, S. Petrushanko, V. Savrin, A. Snigirev

State Research Center of Russian Federation, Institute for High Energy Physics, Protvino, Russia

I. Azhgirey, I. Bayshev, S. Bitioukov, V. Kachanov, A. Kalinin, D. Konstantinov, V. Krychkine, V. Petrov, R. Ryutin, A. Sobol, L. Tourtchanovitch, S. Troshin, N. Tyurin, A. Uzunian, A. Volkov

University of Belgrade, Faculty of Physics and Vinca Institute of Nuclear Sciences, Belgrade, Serbia

P. Adzic³³, M. Ekmedzic, J. Milosevic, V. Rekovic

Centro de Investigaciones Energéticas Medioambientales y Tecnológicas (CIEMAT), Madrid, Spain

J. Alcaraz Maestre, C. Battilana, E. Calvo, M. Cerrada, M. Chamizo Llatas, N. Colino, B. De La Cruz, A. Delgado Peris, D. Domínguez Vázquez, A. Escalante Del Valle, C. Fernandez Bedoya, J.P. Fernández Ramos, J. Flix, M.C. Fouz, P. Garcia-Abia, O. Gonzalez Lopez, S. Goy Lopez, J.M. Hernandez, M.I. Josa, E. Navarro De Martino, A. Pérez-Calero Yzquierdo, J. Puerta Pelayo, A. Quintario Olmeda, I. Redondo, L. Romero, M.S. Soares

Universidad Autónoma de Madrid, Madrid, Spain

C. Albajar, J.F. de Trocóniz, M. Missiroli, D. Moran

Universidad de Oviedo, Oviedo, Spain

H. Brun, J. Cuevas, J. Fernandez Menendez, S. Folgueras, I. Gonzalez Caballero

Instituto de Física de Cantabria (IFCA), CSIC-Universidad de Cantabria, Santander, Spain

J.A. Brochero Cifuentes, I.J. Cabrillo, A. Calderon, J. Duarte Campderros, M. Fernandez, G. Gomez, A. Graziano, A. Lopez Virto, J. Marco, R. Marco, C. Martinez Rivero, F. Matorras, F.J. Munoz Sanchez, J. Piedra Gomez, T. Rodrigo, A.Y. Rodríguez-Marrero, A. Ruiz-Jimeno, L. Scodellaro, I. Vila, R. Vilar Cortabitarte

CERN, European Organization for Nuclear Research, Geneva, Switzerland

D. Abbaneo, E. Auffray, G. Auzinger, M. Bachtis, P. Baillon, A.H. Ball, D. Barney, A. Benaglia, J. Bendavid, L. Benhabib, J.F. Benitez, P. Bloch, A. Bocci, A. Bonato, O. Bondu, C. Botta, H. Breuker, T. Camporesi, G. Cerminara, S. Colafranceschi³⁴, M. D'Alfonso, D. d'Enterria, A. Dabrowski, A. David, F. De Guio, A. De Roeck, S. De Visscher, E. Di Marco, M. Dobson, M. Dordevic, B. Dorney, N. Dupont-Sagorin, A. Elliott-Peisert, G. Franzoni, W. Funk, D. Gigi, K. Gill, D. Giordano, M. Girone, F. Glege, R. Guida, S. Gundacker, M. Guthoff, J. Hammer, M. Hansen, P. Harris, J. Hegeman, V. Innocente, P. Janot, K. Kousouris, K. Krajczar, P. Lecoq,

C. Lourenço, N. Magini, L. Malgeri, M. Mannelli, J. Marrouche, L. Masetti, F. Meijers, S. Mersi, E. Meschi, F. Moortgat, S. Morovic, M. Mulders, L. Orsini, L. Pape, E. Perez, A. Petrilli, G. Petrucciani, A. Pfeiffer, M. Pimiä, D. Piparo, M. Plagge, A. Racz, G. Rolandi³⁵, M. Rovere, H. Sakulin, C. Schäfer, C. Schwick, A. Sharma, P. Siegrist, P. Silva, M. Simon, P. Sphicas³⁶, D. Spiga, J. Steggemann, B. Stieger, M. Stoye, Y. Takahashi, D. Treille, A. Tsirou, G.I. Veres¹⁷, N. Wardle, H.K. Wöhri, H. Wollny, W.D. Zeuner

Paul Scherrer Institut, Villigen, Switzerland

W. Bertl, K. Deiters, W. Erdmann, R. Horisberger, Q. Ingram, H.C. Kaestli, D. Kotlinski, U. Langenegger, D. Renker, T. Rohe

Institute for Particle Physics, ETH Zurich, Zurich, Switzerland

F. Bachmair, L. Bäni, L. Bianchini, M.A. Buchmann, B. Casal, N. Chanon, G. Dissertori, M. Dittmar, M. Donegà, M. Dünser, P. Eller, C. Grab, D. Hits, J. Hoss, W. Lustermann, B. Mangano, A.C. Marini, M. Marionneau, P. Martinez Ruiz del Arbol, M. Masciovecchio, D. Meister, N. Mohr, P. Musella, C. Nägeli³⁷, F. Nessi-Tedaldi, F. Pandolfi, F. Pauss, L. Perrozzi, M. Peruzzi, M. Quitnat, L. Rebane, M. Rossini, A. Starodumov³⁸, M. Takahashi, K. Theofilatos, R. Wallny, H.A. Weber

Universität Zürich, Zurich, Switzerland

C. Amsler³⁹, M.F. Canelli, V. Chiochia, A. De Cosa, A. Hinzmann, T. Hreus, B. Kilminster, C. Lange, B. Millan Mejias, J. Ngadiuba, D. Pinna, P. Robmann, F.J. Ronga, S. Taroni, M. Verzetti, Y. Yang

National Central University, Chung-Li, Taiwan

M. Cardaci, K.H. Chen, C. Ferro, C.M. Kuo, W. Lin, Y.J. Lu, R. Volpe, S.S. Yu

National Taiwan University (NTU), Taipei, Taiwan

P. Chang, Y.H. Chang, Y. Chao, K.F. Chen, P.H. Chen, C. Dietz, U. Grundler, W.-S. Hou, Y.F. Liu, R.-S. Lu, E. Petrakou, Y.M. Tzeng, R. Wilken

Chulalongkorn University, Faculty of Science, Department of Physics, Bangkok, Thailand

B. Asavapibhop, G. Singh, N. Srimanobhas, N. Suwonjandee

Cukurova University, Adana, Turkey

A. Adiguzel, M.N. Bakirci⁴⁰, S. Cerci⁴¹, C. Dozen, I. Dumanoglu, E. Eskut, S. Girgis, G. Gokbulut, Y. Guler, E. Gurpinar, I. Hos, E.E. Kangal, A. Kayis Topaksu, G. Onengut⁴², K. Ozdemir, S. Ozturk⁴⁰, A. Polatoz, D. Sunar Cerci⁴¹, B. Tali⁴¹, H. Topakli⁴⁰, M. Vergili, C. Zorbilmez

Middle East Technical University, Physics Department, Ankara, Turkey

I.V. Akin, B. Bilin, S. Bilmis, H. Gamsizkan⁴³, B. Isildak⁴⁴, G. Karapinar⁴⁵, K. Ocalan⁴⁶, S. Sekmen, U.E. Surat, M. Yalvac, M. Zeyrek

Bogazici University, Istanbul, Turkey

E.A. Albayrak⁴⁷, E. Gülmез, M. Kaya⁴⁸, O. Kaya⁴⁹, T. Yetkin⁵⁰

Istanbul Technical University, Istanbul, Turkey

K. Cankocak, F.I. Vardarli

National Scientific Center, Kharkov Institute of Physics and Technology, Kharkov, Ukraine

L. Levchuk, P. Sorokin

University of Bristol, Bristol, United Kingdom

J.J. Brooke, E. Clement, D. Cussans, H. Flacher, J. Goldstein, M. Grimes, G.P. Heath, H.F. Heath,

J. Jacob, L. Kreczko, C. Lucas, Z. Meng, D.M. Newbold⁵¹, S. Paramesvaran, A. Poll, T. Sakuma, S. Seif El Nasr-storey, S. Senkin, V.J. Smith

Rutherford Appleton Laboratory, Didcot, United Kingdom

K.W. Bell, A. Belyaev⁵², C. Brew, R.M. Brown, D.J.A. Cockerill, J.A. Coughlan, K. Harder, S. Harper, E. Olaiya, D. Petyt, C.H. Shepherd-Themistocleous, A. Thea, I.R. Tomalin, T. Williams, W.J. Womersley, S.D. Worm

Imperial College, London, United Kingdom

M. Baber, R. Bainbridge, O. Buchmuller, D. Burton, D. Colling, N. Cripps, P. Dauncey, G. Davies, M. Della Negra, P. Dunne, W. Ferguson, J. Fulcher, D. Futyan, G. Hall, G. Iles, M. Jarvis, G. Karapostoli, M. Kenzie, R. Lane, R. Lucas⁵¹, L. Lyons, A.-M. Magnan, S. Malik, B. Mathias, J. Nash, A. Nikitenko³⁸, J. Pela, M. Pesaresi, K. Petridis, D.M. Raymond, S. Rogerson, A. Rose, C. Seez, P. Sharp[†], A. Tapper, M. Vazquez Acosta, T. Virdee, S.C. Zenz

Brunel University, Uxbridge, United Kingdom

J.E. Cole, P.R. Hobson, A. Khan, P. Kyberd, D. Leggat, D. Leslie, I.D. Reid, P. Symonds, L. Teodorescu, M. Turner

Baylor University, Waco, USA

J. Dittmann, K. Hatakeyama, A. Kasmi, H. Liu, T. Scarborough, Z. Wu

The University of Alabama, Tuscaloosa, USA

O. Charaf, S.I. Cooper, C. Henderson, P. Rumerio

Boston University, Boston, USA

A. Avetisyan, T. Bose, C. Fantasia, P. Lawson, C. Richardson, J. Rohlf, J. St. John, L. Sulak

Brown University, Providence, USA

J. Alimena, E. Berry, S. Bhattacharya, G. Christopher, D. Cutts, Z. Demiragli, N. Dhingra, A. Ferapontov, A. Garabedian, U. Heintz, G. Kukartsev, E. Laird, G. Landsberg, M. Luk, M. Narain, M. Segala, T. Sinthuprasith, T. Speer, J. Swanson

University of California, Davis, Davis, USA

R. Breedon, G. Breto, M. Calderon De La Barca Sanchez, S. Chauhan, M. Chertok, J. Conway, R. Conway, P.T. Cox, R. Erbacher, M. Gardner, W. Ko, R. Lander, M. Mulhearn, D. Pellett, J. Pilot, F. Ricci-Tam, S. Shalhout, J. Smith, M. Squires, D. Stolp, M. Tripathi, S. Wilbur, R. Yohay

University of California, Los Angeles, USA

R. Cousins, P. Everaerts, C. Farrell, J. Hauser, M. Ignatenko, G. Rakness, E. Takasugi, V. Valuev, M. Weber

University of California, Riverside, Riverside, USA

K. Burt, R. Clare, J. Ellison, J.W. Gary, G. Hanson, J. Heilman, M. Ivova Rikova, P. Jandir, E. Kennedy, F. Lacroix, O.R. Long, A. Luthra, M. Malberti, M. Olmedo Negrete, A. Shrinivas, S. Sumowidagdo, S. Wimpenny

University of California, San Diego, La Jolla, USA

J.G. Branson, G.B. Cerati, S. Cittolin, R.T. D'Agnolo, A. Holzner, R. Kelley, D. Klein, J. Letts, I. Macneill, D. Olivito, S. Padhi, C. Palmer, M. Pieri, M. Sani, V. Sharma, S. Simon, M. Tadel, Y. Tu, A. Vartak, C. Welke, F. Würthwein, A. Yagil

University of California, Santa Barbara, Santa Barbara, USA

D. Barge, J. Bradmiller-Feld, C. Campagnari, T. Danielson, A. Dishaw, V. Dutta, K. Flowers,

M. Franco Sevilla, P. Geffert, C. George, F. Golf, L. Gouskos, J. Incandela, C. Justus, N. Mccoll, S.D. Mullin, J. Richman, D. Stuart, W. To, C. West, J. Yoo

California Institute of Technology, Pasadena, USA

A. Apresyan, A. Bornheim, J. Bunn, Y. Chen, J. Duarte, A. Mott, H.B. Newman, C. Pena, M. Pierini, M. Spiropulu, J.R. Vlimant, R. Wilkinson, S. Xie, R.Y. Zhu

Carnegie Mellon University, Pittsburgh, USA

V. Azzolini, A. Calamba, B. Carlson, T. Ferguson, Y. Iiyama, M. Paulini, J. Russ, H. Vogel, I. Vorobiev

University of Colorado at Boulder, Boulder, USA

J.P. Cumalat, W.T. Ford, A. Gaz, M. Krohn, E. Luiggi Lopez, U. Nauenberg, J.G. Smith, K. Stenson, S.R. Wagner

Cornell University, Ithaca, USA

J. Alexander, A. Chatterjee, J. Chaves, J. Chu, S. Dittmer, N. Eggert, N. Mirman, G. Nicolas Kaufman, J.R. Patterson, A. Ryd, E. Salvati, L. Skinnari, W. Sun, W.D. Teo, J. Thom, J. Thompson, J. Tucker, Y. Weng, L. Winstrom, P. Wittich

Fairfield University, Fairfield, USA

D. Winn

Fermi National Accelerator Laboratory, Batavia, USA

S. Abdullin, M. Albrow, J. Anderson, G. Apolinari, L.A.T. Bauerick, A. Beretvas, J. Berryhill, P.C. Bhat, G. Bolla, K. Burkett, J.N. Butler, H.W.K. Cheung, F. Chlebana, S. Cihangir, V.D. Elvira, I. Fisk, J. Freeman, E. Gottschalk, L. Gray, D. Green, S. Grünendahl, O. Gutsche, J. Hanlon, D. Hare, R.M. Harris, J. Hirschauer, B. Hooberman, S. Jindariani, M. Johnson, U. Joshi, B. Klima, B. Kreis, S. Kwan[†], J. Linacre, D. Lincoln, R. Lipton, T. Liu, J. Lykken, K. Maeshima, J.M. Marraffino, V.I. Martinez Outschoorn, S. Maruyama, D. Mason, P. McBride, P. Merkel, K. Mishra, S. Mrenna, S. Nahm, C. Newman-Holmes, V. O'Dell, O. Prokofyev, E. Sexton-Kennedy, S. Sharma, A. Soha, W.J. Spalding, L. Spiegel, L. Taylor, S. Tkaczyk, N.V. Tran, L. Uplegger, E.W. Vaandering, R. Vidal, A. Whitbeck, J. Whitmore, F. Yang

University of Florida, Gainesville, USA

D. Acosta, P. Avery, P. Bortignon, D. Bourilkov, M. Carver, D. Curry, S. Das, M. De Gruttola, G.P. Di Giovanni, R.D. Field, M. Fisher, I.K. Furic, J. Hugon, J. Konigsberg, A. Korytov, T. Kypreos, J.F. Low, K. Matchev, H. Mei, P. Milenovic⁵³, G. Mitselmakher, L. Muniz, A. Rinkevicius, L. Shchutska, M. Snowball, D. Sperka, J. Yelton, M. Zakaria

Florida International University, Miami, USA

S. Hewamanage, S. Linn, P. Markowitz, G. Martinez, J.L. Rodriguez

Florida State University, Tallahassee, USA

T. Adams, A. Askew, J. Bochenek, B. Diamond, J. Haas, S. Hagopian, V. Hagopian, K.F. Johnson, H. Prosper, V. Veeraraghavan, M. Weinberg

Florida Institute of Technology, Melbourne, USA

M.M. Baarmann, M. Hohlmann, H. Kalakhety, F. Yumiceva

University of Illinois at Chicago (UIC), Chicago, USA

M.R. Adams, L. Apanasevich, D. Berry, R.R. Betts, I. Bucinskaite, R. Cavanaugh, O. Evdokimov, L. Gauthier, C.E. Gerber, D.J. Hofman, P. Kurt, C. O'Brien, I.D. Sandoval Gonzalez, C. Silkworth, P. Turner, N. Varelas

The University of Iowa, Iowa City, USA

B. Bilki⁵⁴, W. Clarida, K. Dilsiz, M. Haytmyradov, J.-P. Merlo, H. Mermerkaya⁵⁵, A. Mestvirishvili, A. Moeller, J. Nachtman, H. Ogul, Y. Onel, F. Ozok⁴⁷, A. Penzo, R. Rahmat, S. Sen, P. Tan, E. Tiras, J. Wetzel, K. Yi

Johns Hopkins University, Baltimore, USA

I. Anderson, B.A. Barnett, B. Blumenfeld, S. Bolognesi, D. Fehling, A.V. Gritsan, P. Maksimovic, C. Martin, M. Swartz

The University of Kansas, Lawrence, USA

P. Baringer, A. Bean, G. Benelli, C. Bruner, J. Gray, R.P. Kenny III, D. Majumder, M. Malek, M. Murray, D. Noonan, S. Sanders, J. Sekaric, R. Stringer, Q. Wang, J.S. Wood

Kansas State University, Manhattan, USA

I. Chakaberia, A. Ivanov, K. Kaadze, S. Khalil, M. Makouski, Y. Maravin, L.K. Saini, N. Skhirtladze, I. Svintradze

Lawrence Livermore National Laboratory, Livermore, USA

J. Gronberg, D. Lange, F. Rebassoo, D. Wright

University of Maryland, College Park, USA

A. Baden, A. Belloni, B. Calvert, S.C. Eno, J.A. Gomez, N.J. Hadley, R.G. Kellogg, T. Kolberg, Y. Lu, A.C. Mignerey, K. Pedro, A. Skuja, M.B. Tonjes, S.C. Tonwar

Massachusetts Institute of Technology, Cambridge, USA

A. Apyan, R. Barbieri, W. Busza, I.A. Cali, M. Chan, L. Di Matteo, G. Gomez Ceballos, M. Goncharov, D. Gulhan, M. Klute, Y.S. Lai, Y.-J. Lee, A. Levin, P.D. Luckey, C. Paus, D. Ralph, C. Roland, G. Roland, G.S.F. Stephans, K. Sumorok, D. Velicanu, J. Veverka, B. Wyslouch, M. Yang, M. Zanetti, V. Zhukova

University of Minnesota, Minneapolis, USA

B. Dahmes, A. Gude, S.C. Kao, K. Klapoetke, Y. Kubota, J. Mans, S. Nourbakhsh, N. Pastika, R. Rusack, A. Singovsky, N. Tambe, J. Turkewitz

University of Mississippi, Oxford, USA

J.G. Acosta, S. Oliveros

University of Nebraska-Lincoln, Lincoln, USA

E. Avdeeva, K. Bloom, S. Bose, D.R. Claes, A. Dominguez, R. Gonzalez Suarez, J. Keller, D. Knowlton, I. Kravchenko, J. Lazo-Flores, F. Meier, F. Ratnikov, G.R. Snow, M. Zvada

State University of New York at Buffalo, Buffalo, USA

J. Dolen, A. Godshalk, I. Iashvili, A. Kharchilava, A. Kumar, S. Rappoccio

Northeastern University, Boston, USA

G. Alverson, E. Barberis, D. Baumgartel, M. Chasco, A. Massironi, D.M. Morse, D. Nash, T. Orimoto, D. Trocino, R.-J. Wang, D. Wood, J. Zhang

Northwestern University, Evanston, USA

K.A. Hahn, A. Kubik, N. Mucia, N. Odell, B. Pollack, A. Pozdnyakov, M. Schmitt, S. Stoynev, K. Sung, M. Velasco, S. Won

University of Notre Dame, Notre Dame, USA

A. Brinkerhoff, K.M. Chan, A. Drozdetskiy, M. Hildreth, C. Jessop, D.J. Karmgard, N. Kellams, K. Lannon, S. Lynch, N. Marinelli, Y. Musienko²⁹, T. Pearson, M. Planer, R. Ruchti, G. Smith, N. Valls, M. Wayne, M. Wolf, A. Woodard

The Ohio State University, Columbus, USA

L. Antonelli, J. Brinson, B. Bylsma, L.S. Durkin, S. Flowers, A. Hart, C. Hill, R. Hughes, K. Kotov, T.Y. Ling, W. Luo, D. Puigh, M. Rodenburg, B.L. Winer, H. Wolfe, H.W. Wulsin

Princeton University, Princeton, USA

O. Driga, P. Elmer, J. Hardenbrook, P. Hebda, S.A. Koay, P. Lujan, D. Marlow, T. Medvedeva, M. Mooney, J. Olsen, P. Piroué, X. Quan, H. Saka, D. Stickland², C. Tully, J.S. Werner, A. Zuranski

University of Puerto Rico, Mayaguez, USA

E. Brownson, S. Malik, H. Mendez, J.E. Ramirez Vargas

Purdue University, West Lafayette, USA

V.E. Barnes, D. Benedetti, D. Bortoletto, M. De Mattia, L. Gutay, Z. Hu, M.K. Jha, M. Jones, K. Jung, M. Kress, N. Leonardo, D.H. Miller, N. Neumeister, F. Primavera, B.C. Radburn-Smith, X. Shi, I. Shipsey, D. Silvers, A. Svyatkovskiy, F. Wang, W. Xie, L. Xu, J. Zablocki

Purdue University Calumet, Hammond, USA

N. Parashar, J. Stupak

Rice University, Houston, USA

A. Adair, B. Akgun, K.M. Ecklund, F.J.M. Geurts, W. Li, B. Michlin, B.P. Padley, R. Redjimi, J. Roberts, J. Zabel

University of Rochester, Rochester, USA

B. Betchart, A. Bodek, R. Covarelli, P. de Barbaro, R. Demina, Y. Eshaq, T. Ferbel, A. Garcia-Bellido, P. Goldenzweig, J. Han, A. Harel, O. Hindrichs, A. Khukhunaishvili, S. Korjenevski, G. Petrillo, D. Vishnevskiy

The Rockefeller University, New York, USA

R. Ciesielski, L. Demortier, K. Goulian, C. Mesropian

Rutgers, The State University of New Jersey, Piscataway, USA

S. Arora, A. Barker, J.P. Chou, C. Contreras-Campana, E. Contreras-Campana, D. Duggan, D. Ferencek, Y. Gershtein, R. Gray, E. Halkiadakis, D. Hidas, S. Kaplan, A. Lath, S. Panwalkar, M. Park, R. Patel, S. Salur, S. Schnetzer, D. Sheffield, S. Somalwar, R. Stone, S. Thomas, P. Thomassen, M. Walker

University of Tennessee, Knoxville, USA

K. Rose, S. Spanier, A. York

Texas A&M University, College Station, USA

O. Bouhali⁵⁶, A. Castaneda Hernandez, R. Eusebi, W. Flanagan, J. Gilmore, T. Kamon⁵⁷, V. Khotilovich, V. Krutelyov, R. Montalvo, I. Osipenkov, Y. Pakhotin, A. Perloff, J. Roe, A. Rose, A. Safonov, I. Suarez, A. Tatarinov, K.A. Ulmer

Texas Tech University, Lubbock, USA

N. Akchurin, C. Cowden, J. Damgov, C. Dragoiu, P.R. Dudero, J. Faulkner, K. Kovitanggoon, S. Kunori, S.W. Lee, T. Libeiro, I. Volobouev

Vanderbilt University, Nashville, USA

E. Appelt, A.G. Delannoy, S. Greene, A. Gurrola, W. Johns, C. Maguire, Y. Mao, A. Melo, M. Sharma, P. Sheldon, B. Snook, S. Tuo, J. Velkovska

University of Virginia, Charlottesville, USA

M.W. Arenton, S. Boutle, B. Cox, B. Francis, J. Goodell, R. Hirosky, A. Ledovskoy, H. Li, C. Lin, C. Neu, J. Wood

Wayne State University, Detroit, USA

C. Clarke, R. Harr, P.E. Karchin, C. Kottachchi Kankanamge Don, P. Lamichhane, J. Sturdy

University of Wisconsin, Madison, USA

D.A. Belknap, D. Carlsmith, M. Cepeda, S. Dasu, L. Dodd, S. Duric, E. Friis, R. Hall-Wilton, M. Herndon, A. Hervé, P. Klabbers, A. Lanaro, C. Lazaridis, A. Levine, R. Loveless, A. Mohapatra, I. Ojalvo, T. Perry, G.A. Pierro, G. Polese, I. Ross, T. Sarangi, A. Savin, W.H. Smith, D. Taylor, C. Vuosalo, N. Woods

†: Deceased

- 1: Also at Vienna University of Technology, Vienna, Austria
- 2: Also at CERN, European Organization for Nuclear Research, Geneva, Switzerland
- 3: Also at Institut Pluridisciplinaire Hubert Curien, Université de Strasbourg, Université de Haute Alsace Mulhouse, CNRS/IN2P3, Strasbourg, France
- 4: Also at National Institute of Chemical Physics and Biophysics, Tallinn, Estonia
- 5: Also at Skobeltsyn Institute of Nuclear Physics, Lomonosov Moscow State University, Moscow, Russia
- 6: Also at Universidade Estadual de Campinas, Campinas, Brazil
- 7: Also at Laboratoire Leprince-Ringuet, Ecole Polytechnique, IN2P3-CNRS, Palaiseau, France
- 8: Also at Joint Institute for Nuclear Research, Dubna, Russia
- 9: Also at Suez University, Suez, Egypt
- 10: Also at Cairo University, Cairo, Egypt
- 11: Also at Fayoum University, El-Fayoum, Egypt
- 12: Also at British University in Egypt, Cairo, Egypt
- 13: Now at Sultan Qaboos University, Muscat, Oman
- 14: Also at Université de Haute Alsace, Mulhouse, France
- 15: Also at Brandenburg University of Technology, Cottbus, Germany
- 16: Also at Institute of Nuclear Research ATOMKI, Debrecen, Hungary
- 17: Also at Eötvös Loránd University, Budapest, Hungary
- 18: Also at University of Debrecen, Debrecen, Hungary
- 19: Also at University of Visva-Bharati, Santiniketan, India
- 20: Now at King Abdulaziz University, Jeddah, Saudi Arabia
- 21: Also at University of Ruhuna, Matara, Sri Lanka
- 22: Also at Isfahan University of Technology, Isfahan, Iran
- 23: Also at University of Tehran, Department of Engineering Science, Tehran, Iran
- 24: Also at Plasma Physics Research Center, Science and Research Branch, Islamic Azad University, Tehran, Iran
- 25: Also at Laboratori Nazionali di Legnaro dell'INFN, Legnaro, Italy
- 26: Also at Università degli Studi di Siena, Siena, Italy
- 27: Also at Centre National de la Recherche Scientifique (CNRS) - IN2P3, Paris, France
- 28: Also at Purdue University, West Lafayette, USA
- 29: Also at Institute for Nuclear Research, Moscow, Russia
- 30: Also at St. Petersburg State Polytechnical University, St. Petersburg, Russia
- 31: Also at National Research Nuclear University "Moscow Engineering Physics Institute" (MEPhI), Moscow, Russia
- 32: Also at California Institute of Technology, Pasadena, USA
- 33: Also at Faculty of Physics, University of Belgrade, Belgrade, Serbia

-
- 34: Also at Facoltà Ingegneria, Università di Roma, Roma, Italy
 - 35: Also at Scuola Normale e Sezione dell'INFN, Pisa, Italy
 - 36: Also at University of Athens, Athens, Greece
 - 37: Also at Paul Scherrer Institut, Villigen, Switzerland
 - 38: Also at Institute for Theoretical and Experimental Physics, Moscow, Russia
 - 39: Also at Albert Einstein Center for Fundamental Physics, Bern, Switzerland
 - 40: Also at Gaziosmanpasa University, Tokat, Turkey
 - 41: Also at Adiyaman University, Adiyaman, Turkey
 - 42: Also at Cag University, Mersin, Turkey
 - 43: Also at Anadolu University, Eskisehir, Turkey
 - 44: Also at Ozyegin University, Istanbul, Turkey
 - 45: Also at Izmir Institute of Technology, Izmir, Turkey
 - 46: Also at Necmettin Erbakan University, Konya, Turkey
 - 47: Also at Mimar Sinan University, Istanbul, Istanbul, Turkey
 - 48: Also at Marmara University, Istanbul, Turkey
 - 49: Also at Kafkas University, Kars, Turkey
 - 50: Also at Yildiz Technical University, Istanbul, Turkey
 - 51: Also at Rutherford Appleton Laboratory, Didcot, United Kingdom
 - 52: Also at School of Physics and Astronomy, University of Southampton, Southampton, United Kingdom
 - 53: Also at University of Belgrade, Faculty of Physics and Vinca Institute of Nuclear Sciences, Belgrade, Serbia
 - 54: Also at Argonne National Laboratory, Argonne, USA
 - 55: Also at Erzincan University, Erzincan, Turkey
 - 56: Also at Texas A&M University at Qatar, Doha, Qatar
 - 57: Also at Kyungpook National University, Daegu, Korea